Estimating canopy gross primary production by combining phloem stable isotopes with canopy and mesophyll conductances

Antoine Vernay, Xianglin Tian, Jinshu Chi, Sune Linder, Annikki Mäkelä, Ram Oren, Matthias Peichl, Zsofia R Stangl, Pantana Tor-Ngern, John D Marshall

Estimating canopy gross primary production by combining phloem stable isotopes with canopy and mesophyll conductances

Edited Version on Plant, Cell and Environment (2020)

Antoine Vernay[1], Xianglin Tian[2], Jinshu Chi[1], Sune Linder[3], Annikki Mäkelä[2], Ram Oren[2,4], Matthias Peichl[1], Zsofia R Stangl[1], Pantana Tor-Ngern[5,6], John D Marshall[1*]

[1]Department of Forest Ecology and Management, Swedish University of Agricultural Sciences (SLU), SE-901 83 Umeå, Sweden

[2]Department of Forest Sciences, University of Helsinki, P.O. Box 27, Helsinki FI-00014, Finland

[3]Southern Swedish Forest Research Centre, SLU, P.O. Box 49, SE-230 53, Alnarp, Sweden

[4]Division of Environmental Science & Policy, Nicholas School of the Environment, and Department of Civil & Environmental Engineering, Pratt School of Engineering, Duke University, Durham, North Carolina, USA

[5]Department of Environmental Science, Faculty of Science, Chulalongkorn University, Bangkok, Thailand

[6]Environment, Health and Social Data Analytics Research Group, Chulalongkorn University, Bangkok, Thailand

* Corresponding author: john.marshall@slu.se, +46-72-248 0477
Number of figures: 5 (figures 3 and 4 are in colour)
Tables: 2
Supporting information: 6 figures (figures 3, 5 and 6 are in colour) and one table

Abstract (195/200)

Gross primary production (GPP) is a key component of the forest carbon cycle. However, our knowledge of GPP at the stand scale remains uncertain because estimates derived from eddy covariance (EC) rely on semi-empirical modeling and the assumptions of the EC technique are sometimes not fully met.

We propose using the sap flux/isotope method as an alternative way to estimate canopy GPP, termed $GPP_{iso/SF}$, at the stand scale and at daily resolution. It is based on canopy conductance inferred from sap flux and intrinsic water-use efficiency estimated from the stable carbon isotope composition of phloem contents. The $GPP_{iso/SF}$ estimate was further corrected for seasonal variations in photosynthetic capacity and mesophyll conductance.

We compared our estimate of $GPP_{iso/SF}$ to the GPP derived from PRELES, a model parameterised with EC data. The comparisons were performed in a highly instrumented, boreal Scots pine forest in northern Sweden, including a nitrogen fertilised and a reference plot.

The resulting annual and daily $GPP_{iso/SF}$ estimates agreed well with PRELES, in the fertilised plot and the reference plot. We discuss the $GPP_{iso/SF}$ method as an alternative which can be widely applied without terrain restrictions, where the assumptions of EC are not met.

Keywords

boreal forest, canopy conductance, gross primary production, intrinsic water-use efficiency, mesophyll conductance, nitrogen fertilisation, phloem $\delta^{13}C$, PRELES, sap flux, stand transpiration

1 | INTRODUCTION

Gross primary production (GPP) represents a key flux in the carbon (C) budget of a forest ecosystem. GPP has been commonly estimated using many approaches, such as eddy covariance (EC), empirical models, and upscaling ecophysiological measurements at stand scale (Baldocchi, 2003; Beer et al., 2010; Peichl, Brodeur, Khomik, & Arain, 2010). However, there are still some uncertainties in these GPP estimates (Campbell et al., 2017). For example, accurate EC estimates are based on a set of assumptions, such as homogeneous flat terrain and turbulent mixing of air (e.g. Baldocchi, 2003). Because the assumptions are not always met, estimates are prone to ~20% uncertainty (Jocher et al., 2017; Keenan et al., 2019; Wehr et al., 2016).

EC data from periods when underlying assumptions are met can be used for the parameterization of a semi-empirical model such as PRELES (PREdict Light-use efficiency, Evapotranspiration and Soil water) to estimate GPP (GPP_{PRELES}) in a given forest ecosystem (Mäkelä et al., 2008; Peltoniemi, Pulkkinen, Aurela, Pumpanen, Kolari, & Mäkelä, 2015). PRELES can subsequently be used for gap-filling the EC data that have been filtered out or are otherwise missing. One of the advantages of PRELES is that it estimates ecosystem fluxes (GPP and evapotranspiration) by using routinely measured weather data. It means that GPP_{PRELES} can be estimated everywhere with no additional measurement than weather conditions (Tian et al., 2020). This approach allows one to go back in time for estimating GPP of the boreal forest in years for which EC are not available (Minunno et al., 2016).

The weakness of GPP estimates from PRELES is that its estimates are often unanchored by methods that are independent of EC. Previous studies that compared between biometric/component fluxes and GPP from EC (GPP_{EC}) data have found that the GPP trends agreed reasonably well over several years, but often failed to find the same absolute values at annual scales (Curtis et al., 2002; Ehman et al., 2002; Peichl, Khomik, & Arain, 2010). These studies underlined two main kinds of errors, one due to EC measurements and the other due to the allometric equations and component fluxes. Thus, neither PRELES, EC nor biometric methods can be considered an absolute standard. A previous study compared EC and dendrometric data and found a good correlation, but the dendrometric data do not provide flux estimates and thus require the development of site specific correlations (Zweifel et al., 2010).

A third, alternative approach for estimating GPP is to scale up tree-level ecophysiological measurements to the stand level. This approach requires the scaling of component fluxes such as leaf photosynthesis or sap flux. For example, the Conductance Constrained Carbon Assimilation model (4C-A) combined sap flux-based stomatal conductance with light-dependent photosynthetic parameters to produce vertically explicit photosynthesis estimates in both single- and multi-species stands (Kim, Oren, & Hinckley, 2008; Schäfer et al., 2003). These parameters were used to estimate the vertically explicit ratio between internal C concentration in the stomatal cavity, (C_i) and atmospheric C concentration (C_a) (C_i/C_a) or, weighted by vertical leaf area distribution, a canopy-scale effective C_i/C_a at diurnal resolution. Although it described photosynthesis well (Schäfer et al., 2003), the method required detailed information on canopy architecture and gas exchange properties, which are not straightforward to obtain. A simpler way forward is to infer intrinsic water use efficiency (WUE_i) from $\delta^{13}C$ (Cernusak et al., 2013; Ehleringer, Hall, & Farquhar, 1993). The $\delta^{13}C$ method avoids the need to measure or assume photosynthetic parameters, as in the 4C-A model. WUE_i represents the ratio between net photosynthesis and the stomatal conductance (g_S) to water vapour (Flexas et al., 2016). It is also equivalent to the CO_2 diffusion gradient between the atmosphere and the substomatal cavity when considering g_S for CO_2 (Farquhar, O'Leary, & Berry, 1982). The WUE_i can be estimated from $\delta^{13}C$ in phloem ($\delta^{13}C_p$) contents, which estimates WUE_i, at the tree scale (Ubierna & Marshall, 2011; Werner et al., 2012). The $\delta^{13}C_p$ measurement integrates the signal from the whole canopy (Rascher, Máguas, & Werner, 2010), and therefore improves on Hu, Moore, Riveros-Iregui, Burns, & Monson (2010), who used a similar approach, but based their $\delta^{13}C$ estimates on sugar extracts from foliage. Rascher, Máguas, & Werner (2010) showed that the $\delta^{13}C$ of water-soluble sugar decreased along the plant axis but to a small extent (~0.8‰). They concluded that $\delta^{13}C_p$ "does provide an integrative measure of changing canopy $\Delta^{13}C$". The whole-tree scale of the calculated WUE_i thus matches the scale of the transpiration estimate.

Some studies using $\delta^{13}C$ to estimate WUE_i (Seibt, Rajabi, Griffiths, & Berry, 2008; Wingate, Seibt, Moncrieff, Jarvis, & Lloyd, 2007) and GPP (Hu et al., 2010; Klein, Rotenberg, Tatarinov, & Yakir, 2016) have highlighted the importance of mesophyll conductance (g_m). The g_m describes the ease with which CO_2 can diffuse from the substomatal cavity to the chloroplasts, where carbon assimilation actually occurs (Flexas, Ribas-Carbó, Diaz-Espejo, Galmès, & Medrano, 2008; Warren & Adams, 2006). Because g_m is finite, assuming that it is infinite leads to an overestimation of WUE_i (Seibt et al., 2008; Wingate et al., 2007). Considering g_m associated with $\delta^{13}C_p$ measurements would considerably improve GPP estimates, especially for conifers, which have relatively low g_m (Rascher, Máguas, & Werner, 2010). There is as yet no agreement about how to model g_m, but it has often been estimated from g_S (Warren, 2008).

We present a new semi-empirical GPP model, hereafter called $GPP_{iso/SF,}$ combining sap flux, $\delta^{13}C_p$, and mesophyll conductance based on approaches developed previously (Hu et al., 2010; Kim et al., 2008; Klein et al., 2016; Schäfer et al., 2003), and compare it to estimates from PRELES. We estimated $GPP_{iso/SF}$ of whole trees at a daily time step and then scaled it up to the stand level. The sap flow/isotopic method would, however, only consider the tree contribution to the ecosystem GPP, in contrast to PRELES, which considers the contribution of the whole ecosystem, including understorey and overstorey species. The understorey contribution from PRELES is in the process of being analysed. However, understorey GPP represents rather little of ecosystem GPP in a closed-canopy boreal forest (Kulmala et al., 2011; Palmroth et al., 2019, Tian et al., 2020. PRELES and the sap flow/isotopic method should therefore give similar results. The $GPP_{iso/SF}$ method can also provide information on how $GPP_{iso/SF}$ responds to fertilisation in terms of assimilation and g_S.

A boreal forest is particularly suited for such a method comparison because of its simple species composition (Hänninen, 2016; Högberg, 2007). Moreover, because this biome is strongly nitrogen (N)-limited (Du et al., 2020), N additions induce a strong response in terms of growth and C fluxes (see reviews and references therein in Högberg, 2007 and Tamm, 1991). These increases should be captured by all methods. However, a positive N-fertilisation effect on GPP was not always observed. At our site, previous studies showed no effect of N supply on GPP when measured from biometrics (Lim et al., 2015) or shoot-scale gas exchange (Tarvainen, Räntfors, Näsholm, & Wallin, 2016), but Tian et al. (2020), who used eddy covariance data to parametrise a model, did find higher GPP in the fertilised plot than in the reference plot. Thus the GPP results have been mixed, depending on which method was used.

The method we propose in this paper aims to provide an alternative stand-scale estimate of GPP that is independent of eddy covariance. Our first objective here was to compare estimates of GPP based on stable isotopes and sap flux against GPP based on PRELES, a process-based model parameterised with eddy covariance data. The second objective was to determine how fertilisation treatment influenced the canopy GPP with the sap flux/isotope method. Finally, the third objective explores alternative methods for incorporating an empirical g_m estimate and how these alternatives influence the GPP estimate.

2 | MATERIALS AND METHODS

2.1 | Experimental site

The study was carried out in a mature ~90 year-old Scots pine forest (*Pinus sylvestris* L.) at Rosinedal, near Vindeln in northern Sweden (64°10' N, 19°45' E) in 2012 and 2013. The site was an even-aged and mono-specific stand, located on sandy soil. Two 15-ha plots were studied; a fertilised plot (F) and a reference plot (R). In both plots, the sparse understory was dominated by Ericaceous shrubs, esp. *Vaccinium myrtillus* (L.) and *Vaccinium vitis-idaea*, (L.) mosses (*Pleurozium schreberi* (Bird.) Mitt.), *Hylocomium splendens* (Hedw.) Shimp, and lichens (*Cladonia spp.)* (Hasselquist, Metcalfe, & Högberg, 2012; Hasselquist, Metcalfe, Marshall, Lucas, & Högberg, 2016). From 2006 through 2011 fertiliser was applied annually in mid-June to the fertilised plot (F) at a rate of 10 g N m^{-2} yr^{-1}, but reduced to 5 g N m^{-2} yr^{-1} in 2012 and thereafter, using Skog-Can fertiliser (Yara, Sweden), containing NH_4 (13.5%), NO_3 (13.5%), Ca (5%), Mg (2.4%), and B (0.2%) (Lim et al. 2015).

2.2 | Environmental data

Environmental data included half-hourly relative humidity (RH, %), photosynthetic photon flux density (PPFD, µmol m^{-2} s^{-1}), ambient temperature (T_a, °C) and soil water content (SWC, m^3 m^{-3}), and precipitation (mm) (Figure S1). PPFD was measured at the R plot only and precipitation came from Svartberget station, which is located about 8 km from the study site. During the period 1981-2010, mean annual temperature and precipitation at Svartberget was 1.8 °C and 614 mm, respectively (Laudon et al., 2013). Gaps in the meteorological data, due to instrument failure, were filled using measurements from the Svartberget forest. All abbreviations, their units, and values of constants are summarised in Table 1.

The temperature data were used to define the "thermal growing season" which estimates the period theoretically suitable for vegetation growth for a given year (Cornes, van der Schrier, & Squintu, 2019; Linderholm, 2006). The thermal growing season was defined to begin after the occurrence of five consecutive days with mean daily temperature > 5 °C and the end was defined as the occurrence of five consecutive days < 5 °C (Mäkelä et al., 2006). According to this definition, the 2012 growing season lasted from 14th of May to 10th of October and, in 2013, from 8th of May to 14th of October.
Atmospheric CO_2 concentration and $\delta^{13}C$ ($\delta^{13}C_a$, ‰) were both collected from the National Oceanic and Atmospheric Administration database using the nearest sample station, at Pallas-Sammaltunturi in Finland (White, Vaughn, & Michel, 2015). This was necessary to account for pronounced seasonal and annual variation in these variables at our high latitude.

2.3 | Measurements of $\delta^{13}C_p$

We measured the $\delta^{13}C$ of the solutes in the fluid moving through the phloem ($\delta^{13}C_p$, ‰). Phloem samples were collected at breast height on 15 tree trunks in each plot with a cork-corer 9 mm in diameter. The samples were collected on 18 October 2011 and 11 November 2011 and then every 14 days from 26 April to 25 September, 2012. In the field, bark and wood were carefully removed and a disc, which included the active phloem, was dropped into a 6 mL vial containing 2 mL of exudation solution (15 mM polyphosphate buffer: sodium hexametaphosphate, Sigma, München, Germany). The solution was chosen to minimise the blockage of cut phloem cells without adding carbon to the exudate solution. The exudation lasted for 5 hours (Gessler, Rennenberg, & Keitel, 2004) and the exudate was then stored in a freezer until it was freeze-dried. Because the phloem solute concentration is much higher than in adjacent tissues, the exudate was dominated by phloem sap (Schneider et al., 1996), but some metabolites from living tissues might contaminate the phloem sample despite the careful preparation of the samples. The solutes were redissolved in 150 µL and the resulting solution was pipetted into a tin capsule and dried at 60 °C for 12 hours. The samples were then loaded into an elemental analyser (NA 2500; CE Instruments, Milan, Italy) coupled to an isotope ratio mass spectrometer (Delta Plus; Finnigan MAT GmbH, Bremen, Germany) for $\delta^{13}C$ analysis. The analysis were performed at the SLU stable isotope laboratory (SSIL, Umeå, Sweden, www.slu.se/en/departments/forest-ecology-management/ssil). Isotopic results were expressed in ‰ relative to VPDB (Vienna Pee Dee Belemnite). Amounts of carbon varied depending on the phloem contents at time of sampling, but they ranged from 400 to 1400 µg. The isotopic data were compared to reference standards calibrated against IAEA-600, IAEA-CH-6, and USGS40.

2.4 | Transpiration and canopy conductance estimates

We used the canopy transpiration model of Tor-Ngern et al. (2017) to avoid the need to repeat their scaling from trees to canopy. The model was originally derived using the measurements at the two plots in Rosinedal. Per-tree transpiration rates were derived from sap flux measured with Granier thermal dissipation probes (Granier, 1985, 1987;) set in five to eight mature trees at varying depths in both the R and F plots (data and methods in Tor-Ngern et al. (2017)). Tree daily transpiration (E_{cd}, mm d^{-1} $tree^{-1}$) was then upscaled to stand level.

The stand-level transpiration estimates were modeled from VPD_Z and relative extractable water (REW). VPD_Z is the integral of daytime mean atmospheric vapour pressure deficit. To estimate it, we first defined daytime as the period when PPFD exceeded a threshold of 10 µmol m^{-2} s^{-1} (Hultine et al., 2008).

VPD_D was then calculated (Murray, 1967; Ngao, Adam, & Saudreau, 2017) for the daylight period, as follows:

$$VPD_D = 0.6108 \times e^{\frac{17.27 \times T_a}{T_a + 237.3}} \times (1 - \frac{RH}{100}) \quad \text{Eqn. 1}$$

Second, VPD_D (kPa) was integrated over the number of daylight hours (Oren, Zimmermann, & Terbough, 1996):

$$VPD_Z = VPD_D \times \frac{n_D}{24} \quad \text{Eqn. 2}$$

with n_D being the number of daylight hours. VPD_Z thus combines daytime VPD and daylength in a single variable.

REW was calculated at 15 cm depth as follows (Granier, Loustau, & Bréda, 2000):

$$REW = \frac{SWC_t - SWC_{WP}}{SWC_{FC} - SWC_{WP}} \quad \text{Eqn. 3}$$

where SWC_t is the mean volumetric soil water content (m^3 m^{-3}) per day. SWC was measured with reflectometric soil moisture probes (SM300, Delta-T Devices, Cambridge, UK) at 15cm depth. SWC_{WP} and SWC_{FC} are the soil water content at wilting point and field capacity, respectively. They were estimated from the annual minimum and maximum SWC, respectively, at our sites. The minimal SWC was used as a proxy of SWC_{WP} because it was similar to a three-year observations during drying cycle on our sandy site and close to the wilting point in a sand (Kätterer, Andrén,& Jansson, 2006; Tor-Ngern et al., 2017). For the F plot, SWC_{WP} and SWC_{FC} were 0.052 and 0.306 m^3 m^{-3}, respectively, and for the R plot, the values were 0.052 and 0.218 m^3 m^{-3}. The F plot had a higher SWC_{FC} value because the soil organic layer was deeper than in the R plot (Hasegawa et al., personal communication).

Using the parameters above, the model of stand-level transpiration rate begins with an estimate of the maximal transpiration rate (E_{cdmax}). It then adjusts the maximum rate downward for REW, as follows:

$$E_{cdmax} = 1.812 \times (1 - e^{-3.121 \times VPDz}) \quad \text{Eqn. 4}$$

$$E_{cd} = E_{cdmax} \times (1 - e^{-18.342 \times REW}) \quad \text{Eqn. 5}$$

Eqn. 4 means that the maximal E_{cdmax} is 1.812 mm d^{-1} at high VPD_Z. It describes the net effect of increasing VPD as the driving force for transpiration and decreasing stomatal conductance as VPD rises (Marshall & Waring, 1984; Oren, Philipps, Ewers, Pataki, & Megonigal, 1999). Equation 5 describes the further reduction that occurs as the soil dries.

Canopy conductance to H_2O was then inferred from corresponding E_{cd} and VPD_D as:

$$g_C = \frac{\frac{E_{cd}}{M_{H2O}} \times 1000}{\frac{VPD_D}{P_{145}}} \quad \text{Eqn. 6}$$

in mol H_2O m^{-2} ground area d^{-1} with M_{H2O} the molar mass of water (18 g mol^{-1}) and P_{145}, the atmospheric pressure at 145 m a.s.l (99.6 kPa). There is some circularity in this approach because VPD appears both in the estimation of E_{cdmax} and g_C. Long experience with these models, including tests against water-balance closure, have shown that the approach works (Tor-Ngern et al., 2017).

We applied two filters and one correction to these conductance data. First, we accounted for the acclimation of photosynthetic capacity to air temperature (Mäkelä, Hari, Berninger, Hänninen, & Nikinmaa, 2004). We did this because of the tight coupling of photosynthesis and stomatal opening (Farquhar & Wong, 1984; Medlyn et al., 2011; Tuzet, Perrier, & Leuning, 2003), which allows us to

account for the low stomatal conductance during the wintertime. Photosynthetic capacity $\hat{A}$, (called $\hat{\alpha}$ in the original paper, Mäkelä et al., 2004) was estimated as follows:

$$\hat{A} = \max\{c_1 \times S(t) - S_0, 0\} \quad \text{Eqn. 7}$$

where c_1 a coefficient of proportionality (0.0367 m^3 mol^{-1} °C), S(t) is the state of photosynthetic acclimation (°C) at time t, and S_0 a threshold value of the state of acclimation (-5.33 °C). S(t) was obtained on daily time scale in two steps:

- $$\Delta S(t) = \frac{T_a(t) - S_t}{\tau} \quad \text{Eqn. 8}$$

Where $T_a(t)$ is daily mean temperature on day t and τ the time constant (8.23 days)

- $$S(t+1) = S(t) + \Delta S(t) \quad \text{Eqn. 9}$$

This model describes the linear increase in photosynthetic capacity with temperature in boreal conifers. We corrected our g_C values as follows (Mäkelä et al., 2008):

$$g_{C\hat{A}} = \frac{\hat{A}}{\hat{A}_{max}} \times g_C \quad \text{Eqn. 10}$$

with $\hat{A}_{max}$ the mean value of $\hat{A}$ when photosynthetic capacity was maximal. For $\hat{A}_{max}$, we used the averages from July of 2012 and 2013. July was chosen because temperatures and PPFD were both high and the canopy was presumably near its photosynthetic capacity throughout this period.

Recall that g_c was estimated from VPD_D (Eqn. 6). Because VPD_D was in the denominator and approached zero in early spring, the estimates of g_C were often noisy at that time. Therefore, we filtered and removed all VPD_D values < 0.1 kPa. During the summer time (June-August) the filter threshold was increased to 0.25 kPa. The higher transpiration rate and a longer day-light period during summer created uncertainty in the g_C calculation (Emberson, Wieser, & Ashmore, 2000; Tarvainen, Räntfors, & Wallin, 2015), but we reduced the summer filter threshold to the minimum that would allow us to keep as many data as possible. We filled the resulting GPP gaps using a predictive model ($g_C = a \times \hat{A} + b$) with a and b determined for each combination of treatments. We replaced the $GPP_{iso/SF}$ outliers (beyond the 95% confidence interval of the predicted values) and filtered values by the predicted functions only during the thermal growing season. We did this because the common gapfill functions are based on EC data and we wished to maintain our independence from EC data. The gaps were much larger outside the thermal growing season than within it; because tree photosynthesis is reduced during that time we chose not to fill these gaps.

2.5 | Carbon, discrimination, intrinsic water use efficiency and GPP calculations

Using the phloem samples collected between October 2011 and September 2012, we estimated isotopic discrimination against ^{13}C (Δ, ‰), assuming it was mainly constituted from photosynthetic carbohydrates. It was calculated as follows:

$$\Delta = \frac{\delta^{13}C_a - \delta^{13}C_p}{1 + \frac{\delta^{13}C_p}{1000}} \quad \text{Eqn. 11}$$

We fitted linear interpolations (Figure S2) to determine a daily value of Δ. This step allowed us to estimate $GPP_{iso/SF}$ at a daily time scale. We assumed a constant diel value of Δ. There is evidence of diel fluctuations in Δ (Brandes et al., 2006; Gessler, Tcherkez, Peuke, Ghashghaie, & Farquhar, 2008), but they are rather small, especially in the lower stem. Rascher, Maguas, & Werner (2010) did not find any significant diel variation studying *Pinus pinaster*. Because our purpose was to estimate GPP during the whole year at stand level, we argue that this short term variability would average out over the growing season. The literature also describes variation in Δ between leaves and phloem contents and among compounds in the phloem; we address this variation in the Discussion.

The intrinsic water use efficiency for the stand (WUE_i) was then inferred from the following equation, in each plot:

$$WUE_i = \frac{C_a}{r} \times \frac{b - \Delta - f \times \frac{\Gamma^*}{C_a}}{b - a_a + (b - a_i) \times \frac{g_{C\hat{A}}}{g_m}} \quad \text{Eqn. 12}$$

where C_a is the atmospheric CO_2 concentration (µmol mol^{-1}), r the ratio of diffusivities of water vapour relative to CO_2 in air (1.6), b the fractionation during carboxylation (29‰), *f* the fractionation during photorespiration (16.2‰, Evans & Caemmerer, 2013), a_a and a_i the fractionations of the diffusion through air (4.4‰) and the fractionation of diffusion and dissolution in water (1.8‰), respectively, and g_m the mesophyll conductance (mol CO_2 m^{-2} d^{-1}). The CO_2 compensation point (Γ*, µmol mol^{-1}), was calculated according to the following formula (Medlyn et al., 2002):

$$\Gamma^* = 42.75 \times e^{\frac{37830 \times (T_K - 298)}{298 \times T_K \times R}} \quad \text{Eqn. 13}$$

with T_K the ambient temperature (K) and R the universal gas constant (8.314 J mol^{-1} K^{-1}).

Eqn. 12 did not account for daytime respiration despite the effect it could have on ^{13}C discrimination (Keenan et al., 2019; Tcherkez et al., 2017). However, a recent study proposed an improved model of carbon isotope discrimination; the daytime respiration (R_d) would have an effect on lipids or amino-acids biosynthesis, especially at low assimilation (A) rate, but not on the carbohydrates that would be loaded into the phloem (Busch, Holloway-Phillips, Stuart-Williams, & Farquhar, 2020). Moreover, the phloem contents are dominated by photosynthate produced when A/R_d is high. Under these conditions, the respiration effect is small (Barbour, Ryazanova, & Tcherkez, 2017; Tcherkez et al., 2017). This agrees with observed Δ*e*, the respiratory discrimination effect, by Stangl et al. (2019), which averaged only 0.13‰ at our site. Including this value in the WUE_i calculation would increase WUE_i by 1.5 ± 0.2% and 1.6 ± 0.1% in the F and the R plots, respectively. Because this is well within the error, we have neglected this effect in the current study. Finally, there remain questions about the age of respiratory substrate and the size of the reduction in respiration in the daytime. These considerations lead us to the conclusion that the most parsimonious approach to modeling phloem contents was to neglect the respiration effect. We also used the $\delta^{13}C_p$ from 2012 to estimate WUE_i for the same dates in 2013, assuming that WUE_i was mainly affected by $g_{C\hat{A}}$ and its link with VPD_D and not by the absolute values of $\delta^{13}C_p$. Similarly, we estimated Δ in October and November 2012 and 2013 based on the 2011 measurements of $\delta^{13}C_p$. WUE_i was then calculated on a daily time scale, based on the daily-modeled values of Δ.

Gross primary production (g C m^{-2} ground area d^{-1}) was then calculated from Eqn. 10 and Eqn. 12:

$$GPP_{iso/SF} = WUE_i \times g_{C\hat{A}} \times \frac{M_C}{10^6} \quad \text{Eqn. 14}$$

with M_C the molar mass of C (12 g mol^{-1}). The definitions of Wohlfahrt and Gu (2015) distinguish between "canopy net photosynthesis," which includes carboxylation, respiration, and photorespiration, "canopy apparent photosynthesis," which includes only carboxylation and photorespiration, and "true photosynthesis," which includes carboxylation only. They point out that the flux-partitioning algorithms used to calculate "GPP" with eddy-flux data are intended to estimate apparent photosynthesis (Wohlfahrt & Gu, 2015). The sap flux/isotopic estimate also provides an estimate of canopy apparent photosynthesis, at least in theory, because respiration is not allowed to influence the photosynthate pools loaded into the phloem. However, Wohlfahrt and Gu (2015) go on to note that the flux-partitioning used with eddy-flux data is inexact because it neglects the reduction in leaf respiration in the light. It is beyond the scope of the current manuscript to solve that problem, but we hope that it can be addressed in the near future.

2.6 | g_m assumptions

We used three different assumptions to obtain g_m values:

- (i) constant $g_m/g_{C\hat{A}} = 2.67$. This approach allowed the g_m estimate to vary during the growing season.
- (ii) constant g_m. This value was determined during several summer days, but was used throughout the year.
- (iii) infinite g_m ($g_{m\infty}$), meaning that in Eqn. 12, the $\frac{g_{C\hat{A}}}{g_m}$ term tends to 0.

The values for $g_m/g_{C\hat{A}} = 2.67$ and a constant $g_m = 0.31$ mol CO_2 m^{-2} s^{-1} were calculated from discrimination against ^{13}C measured at our site with a Picarro isotopic CO_2 analyser (G2131-I, Picarro Inc., California, USA) and standard gas exchange according to Stangl et al. (2019).

2.7 | PRELES model

We used the PRELES model to derive GPP_{PRELES} for 2012 and 2013. The model was first parameterised using a Bayesian approach (e.g. Minunno et al., 2016; Tian et al., 2020) for Rosinedal with EC data available from 2014 to 2017 (Jocher et al., 2017). The model was run with environmental data measured on site (temperature, VPD, PPFD, and precipitation) in 2012 and 2013. Canopy leaf area index (LAI) was estimated in 2011 - 2013 (Lim et al., 2015), excluding understorey vegetation. The model predicts GPP at the stand level (Peltoniemi et al., 2015) and thus provides our best estimate of the year when the phloem samples were collected. We implemented PRELES with the daily mean of these data to get an estimation of GPP_{PRELES} in both R and F stands. It provided a comparison against our GPP calculations for 2012 and 2013.

2.8 | Model comparisons

To compare the PRELES estimates for 2012 and 2013 to the $GPP_{iso/SF}$ estimate, we first chose to calculate $GPP_{iso/SF}$ based on $g_m/g_{C\hat{A}} = 2.67$ (Stangl et al., 2019). The constant ratio assumption is widely used in the literature (Klein et al., 2016; Seibt et al., 2008). Second, we tested the $GPP_{iso/SF}$ estimate in the F plot against the R plot. Finally, the annual sums were calculated and compared for $GPP_{iso/SF}$ and GPP_{PRELES} in 2012 and 2013. We combined 2012 and 2013 in order to estimate the inter-annual variability of the different approaches. The standard deviation (SD) was calculated from the mean annual sum in 2012 and 2013.

2.9 | Statistics

There was no replicate of the R and F treatments so it was impossible to perform analyses of variance to infer any fertilisation effect. However, we could not ignore the effect of the fertilisation on the F plot (Lim et al., 2015). We therefore presented the plot differences recognising that they may include a pre-existing plot effect as well as a fertiliser effect.

However, because 15 trees were sampled at each site for $\delta^{13}C_p$ estimate, we did analyse a 'plot effect'. We performed the same analyses of variance with WUE_i which could be estimated for all of the 15 trees at each date. When necessary, $\delta^{13}C_p$ and WUE_i data were log-transformed to meet normality and homoscedasticity requirements. Temporal variations of $\delta^{13}C_p$ and WUE_i were analysed with a linear mixed model to take into account the repeated $\delta^{13}C_p$ sampling within individual trees in 2012. 'Sampling date', 'plot' and 'plot × sampling date' were assigned as fixed factors whereas the 'tree identity' was considered as a random factor. Similarly, we determined the variance between the different annual sums of $GPP_{iso/SF}$ (according to the three g_m assumptions) and with GPP_{PRELES}: 'plot' and 'method' (three g_m assumptions + PRELES) factors were tested on the mean value in 2012-2013. Daily GPP regressions were run with a first-order autoregressive structure, applying the corAR1correlation option. The analyses were performed with R nlme package (Pinheiro, Bates, DebRoy, & Sarkar, 2016). The anova function from 'car' library and multiple pairwise comparisons (library 'lsmeans' and 'multcompView') were performed.

Finally, we applied a Monte Carlo method to analyse the error propagation in our $GPP_{iso/SF}$ model. This approach was already used in a previous study estimating GPP over a few days (Hu et al., 2010). We

randomly sampled from the uncertainty ranges of Δ, E_{cd}, and $g_m/g_{C\hat{A}}$ to calculate $GPP_{iso/SF}$ in an iterative manner (1000 times). The seasonal pattern of Δ was modeled with the loess method (Cleveland, Grosse, & Shyu, 1992). The uncertainty of daily Δ was estimated based on the residual variance in the curve fitting. Uncertainty of E_{cd} (from Eqn 4 and 5) was calculated based on the original regression analysis of the transpiration model in Tor-Ngern et al. (2017). Uncertainty of $g_m/g_{C\hat{A}}$ was estimated based on the field measurements in Stangl et al. (2019). Uncertainty of Γ* (from Eqn. 13) was estimated based on the mismatches in the original model fitting in Bernacchi, Singsaas, Pimentel, Portis Jr, & Long (2001). Errors in those inputs were assumed to follow normal distributions or truncated normal distributions (see Table S1). The 95% confidence intervals were calculated to illustrate the predictive uncertainty in our $GPP_{iso/SF}$ estimate (Figure S3). The Sobol indices (Saltelli et al., 2008) were also calculated to partition the variance into these uncertainty sources (Table S1). This method allows us to deal with the absence of replicate sites.

Using Bayesian calibration, we adjusted parameters of PRELES according to their ability to reproduce EC observations (Tian et al., 2020). The Bayesian framework treated all terms in the model calibrations and predictions as probability distributions (Clark, 2007; Dietze, 2017). The joint posterior distribution of parameters was obtained using Markov chain Monte Carlo sampling techniques (Hastings, 1970; Metropolis, Rosenbluth, Rosenbluth, Teller, & Teller, 1953). Meanwhile, the probability density distribution of measurement error was estimated. Based on the parametric uncertainty from the joint posterior distribution and the measurement uncertainty from the error distribution, we estimated the 95% confidence intervals of daily GPP predictions, which describes the ranges of eddy covariance observations that could possibly occur.

All analyses were conducted with R software, version 3.5.1 (R Core Team, 2016).

3 | RESULTS

3.1 | Environmental data

We first present seasonal variations of the precipitation, PPFD, temperature and VPD_Z in 2012 and 2013, which were typical of boreal forests (Figure S1). The annual mean temperature during 2012 and 2013 was 1.6 °C and 3.3 °C, and the total precipitation 796 mm and 542 mm, respectively. Precipitation was relatively high during the thermal growing season limiting the potential for drought during the growth period. The light level increased almost three months before the start of the thermal growing season and the maximum values were in June before they decreased until winter. The temperatures were the highest in July-August and reached very low values in winter. Temperatures stayed below zero for several months. Finally, VPD_Z was highest during the thermal growing season although its increase started around March for both years. VPD_Z showed high variability over the whole year.

3.2 | Stand canopy conductance

Stand conductance, $g_{C\hat{A}}$, is an important component of the estimation of $GPP_{iso/SF}$. Stand conductance showed strong seasonal trends with no difference between the F and the R plot (Figure 1). $g_{C\hat{A}}$, started to increase in both plots on March 12th in 2012 and on April 14th in 2013. The difference was due to low temperatures in March 2013 compared to 2012. The winter and fall periods rarely showed any positive conductance because the VPD and $\hat{A}$ corrections filters forced the values to zero. Rates were highest from early June until the beginning of September, which is the core of the thermal growing season. During this period the ratio $\hat{A}/\hat{A}_{max}$ was close to 1 (Figure S4) meaning that photosynthetic capacity had reached its seasonal maximum (Mäkelä et al., 2008). Conductance fell through September and October, returning to zero in both plots on the 25th of October in 2012 and the 4th of December in 2013 (Figure 1).

3.3 | Isotopic data

Isotopic data from the atmosphere and from the phloem were also used to infer WUE_i. We observed strong, but different, patterns of seasonal variation for atmospheric $\delta^{13}C_a$ and for phloem contents ($\delta^{13}C_p$). From January to the beginning of February, $\delta^{13}C_a$ decreased to a minimum of -9.2‰ (Figure 2-

A). Then $\delta^{13}C_a$ increased rapidly, by about 1‰, during the initial weeks of high photosynthesis in late June and early July. The main peaks of $\delta^{13}C_a$ occurred during the thermal growing season, when canopy conductance was also the highest. It then stabilised until late September, when it again began to fall (Figure 2-A). In contrast, the phloem data (Figure. 2-B) did not simply track the atmosphere. Instead they showed a steep drop only at the beginning of the thermal growing season. The $\delta^{13}C_p$ value depended significantly on the date (p-value < 0.0001, df = 1, F = 53.09, Figure 2-B). It was significantly higher in the F plot (-27.5‰) than in the R plot (-28.0‰) (p-value < 0.0001, df = 1, F = 76.96) as well.

3.4 | Intrinsic water use efficiency (WUE_i)

WUE_i is a key variable in the $GPP_{iso/SF}$ estimation procedure (Figure 3). For all three g_m assumptions, WUE_i showed a significant seasonal pattern ('date' effect, p-value < 0.0001, df = 1, F = 29), decreasing sharply as the thermal growing season began and increasing as it ended (Figure 3). WUE_i also decreased gradually over the summer. In 2012, the mean values on the fertilised plot were 6% higher for $g_{m\infty}$, 7% higher for $g_m/g_{C\hat{A}} = 2.67$, and 9% higher for, $g_m = 0.31$ mol CO_2 m^{-2} s^{-1} respectively. In 2013, the relative increase in WUE_i on the F plot was similar: 6%, 7% and 8% respectively. For both years, there was a significant 'plot' effect (p-value < 0.0001, df = 1,) and a significant effect of the g_m assumptions (p-value < 0.0001, df = 2) (Figure 3).

3.5 | Comparison of GPP estimates

Our first objective was to compare $GPP_{iso/SF}$ to GPP_{PRELES} for 2012 and 2013. To simplify the figure, we chose to represent only the assumption that $g_m/g_{C\hat{A}} = 2.67$ (Figure 4), which allows g_m to vary during the season. The seasonal GPP patterns were similar between PRELES and the sap flux/isotopic method (Figure 4). Recall that GPP_{PRELES} included understorey vegetation. Correlation coefficients among methods and plots were all high, with minimum r = 0.91 (Figure S5). However, the fit was nonlinear; in 2012 and 2013 $GPP_{iso/SF}$ approached an asymptote at high levels of GPP_{PRELES} (Figure S5). The highest GPP_{PRELES} values did not match with the highest $GPP_{iso/SF}$ values; the peak of $GPP_{iso/SF}$ occurred earlier in the season than those of GPP_{PRELES}. Interestingly, confidence intervals for $GPP_{iso/SF}$ and GPP_{PRELES} overlapped most of the time, even during the fall, when the offset was bigger than the rest of the year. However, the VPD filters removed many values during the fall, which allowed us to draw a confidence interval only during small periods at that time. As previously mentioned, the GPP values were gapfilled to draw a complete seasonal pattern, at least during the thermal growing season. The resulting annual sums were higher for $GPP_{iso/SF}$ than for PRELES on the control plot, but not on the fertilised plot (Figure 5-A).

3.6 | Fertilisation effect

Our second objective was to assess the effect of fertilisation on GPP. Using the annual sums, neither $GPP_{iso/SF}$ nor GPP_{PRELES} was significantly different between the F and the R plots (Figure 5-A). However, there were consistent trends; $GPP_{iso/SF}$ was higher by 10% in the F plot than in the R plot and GPP_{PRELES} was higher by 16% (Figure 5-A). Using the daily data corrected for autocorrelation, we found a significant increase in the F plot; $GPP_{iso/SF}$ was higher by 8% and GPP_{PRELES} was higher by 16% (Table 2 and see Figure S6).

3.7 | Mesophyll conductance assumptions

The third objective was to compare $GPP_{iso/SF}$ using different methods of estimating g_m. Globally, there was a significant effect of 'plot' (p-value = 0.007, df = 5, F = 19) and 'g_m assumptions' (p-value = 0.0002, df = 5, F = 75). Focusing on one plot at a time, we found a significantly lower $GPP_{iso/SF}$ in the control plot estimates when using $g_m/g_{C\hat{A}} = 2.67$ as compared to the others. In the fertilised plot, we found significantly lower $GPP_{iso/SF}$ of $g_m/g_{C\hat{A}} = 2.67$ compared to $g_{m\infty}$. The F plot was not significantly different from the R plot by any of these methods (Figure 5-B).

4 | DISCUSSION

Our study provided a new and simple method of independently estimating GPP and compared it to estimates from PRELES, a model parameterised with EC data. The two methods yielded similar estimates for both annual totals and seasonal patterns. We then used the two methods to compare a

fertilised to an unfertilised plot. Both methods detected higher GPP on the F plot, but only when using the more abundant daily estimates (Table 2, Figure S5).

Several previous studies have estimated GPP from Scots pine forests in northern Europe. Such EC estimates include 1001 g C m^{-2} y^{-1} (Magnani et al., 2007), 940 g C m^{-2} y^{-1} (Kolari, Pumpanen, Rannik, Ilvesniemi, Hari, & Berninger, 2004), 1047 g C m^{-2} y^{-1} (Lagergren et al., 2008), and 1072 g C m^{-2} y^{-1} (Duursma et al., 2009). There have been two estimates that were independent of EC. The first was a chamber-based estimate of 982 g C m^{-2} y^{-1} (Zha, Xing, Wang, Kellomäki, & Barr, 2007). The second, based on earlier measurements of NPP at our site, was ~1000 g C m^{-2} y^{-1} (Lim et al., 2015). We compared our $GPP_{iso/SF}$ estimate minus our standard deviation for the reference plot (1350 - 43 = 1303 g C m^{-2} y^{-1}) to the mean of these published values plus the standard deviation (1007 + 43 = 1050 g C m^{-2} y^{-1}) and found that the published values were consistently lower than our $GPP_{iso/SF}$ estimate. We next discuss the strengths and weaknesses of each method.

4.1 | Strengths and weaknesses of PRELES

The key advantage of PRELES is that it is a compromise between predictive accuracy and model complexity. It can be calibrated with a few variables derived from EC measurements. Once it is calibrated, it can be run with an even smaller set of environmental variables (VPD, PPFD, precipitation and air temperature). The required EC data are available from many sites around the world (Baldocchi, 2003). PRELES has been reported to work well in all boreal forests (Minunno et al., 2016, Tian et al., 2020). Based on this assessment, we felt justified in using it, with calibration from 2014-2017 and environmental data from 2012-2013, to model carbon fluxes in 2012-2013.

Although the availability of EC data is an advantage for PRELES, EC data must be viewed with caution. In particular, at our site, preliminary analyses of the data revealed significant problems in the data despite the flat ground surface, uniform canopy, and low leaf area index. A careful study of the problem revealed significant decoupling of the above- and below-canopy air masses, which often led to advection (Jocher et al., 2018). It is common for EC studies to use a vertical wind speed cutoff, the u* filter, to detect and remove such events (Aubinet et al., 2001; Papale et al., 2006). We found that the u* filter was insufficient and that a measurement relying on the comparison of below-canopy and above-canopy vertical wind speeds was required (Jocher et al., 2018). This concern was earlier raised in another boreal forest in Finland (Alekseychik, Mammarella, Launiainen, Rannik, & Vesala, 2013). We used a decoupling filter (Thomas, Martin, Law, & Davis, 2013), which is still unusual in the EC community, to correct the EC data that were used to parametrize PRELES in this study. Unless this correction was performed, PRELES would have been parameterised incorrectly if we wished to quantify total ecosystem fluxes; it would only have described the decoupled fluxes.

4.2 | Strengths and weaknesses of sap flux/isotopic approach

4.2.1 | Combination of sap flux and isotopic measurements.

The key advantage of the sap flux/isotopic approach is that it is independent of eddy covariance. Moreover, it leans on two methods, sap flux (Poyatos et al., 2007) and isotopic measurements (Bowling, Pataki, & Randerson, 2008 and references therein) that have been widely used at many sites by ecosystem ecologists. The sap flux/isotopic approach combines them to estimate GPP at the tree scale, which can then be scaled up to the stand. In simple stand structures, that scaling is relatively easy. We used a model of sapflux based on measurements at our site scaled up in this way. It provided a simple method to estimate tree GPP that, in combination with measurements of ground vegetation GPP, yields an alternative estimate for comparison with GPP estimated by EC.

One critical advantage of the sap flux/isotopic method for estimating GPP is that its requirements for the terrain and atmospheric conditions are less restrictive than for EC measurements. It thus provides an empirical method that can be applied in hilly topography, complex canopy structure, and non-turbulent atmospheres.

4.2.2 | Phloem contents and isotopic interpretation

The sap flux/isotopic method also has several important limitations. The literature describes several post-photosynthetic modifications in the isotopic composition of the carbon that appears in the phloem

(Cernusak et al., 2009), which might interfere with our interpretation of the phloem contents as representative of the photosynthate, and finally with our WUE_i estimates (Brandes et al., 2006; Dubbert, Rascher, & Werner, 2012; Gessler, Tcherkez, Peuke, Ghashghaie, & Farquahr, 2008; Merchant et al., 2012). Especially pronounced are the modifications that occur when the beta-oxidation pathway is activated, as when lipids and lignin are produced. These modifications are especially strong when lipid or lignin concentrations are high, as in bulk leaf tissue (Bowling et al., 2008). However, lipids and lignin are not abundant in phloem contents because their function is not related to transport and they are largely insoluble in water. In fact, their near absence would suggest that phloem contents are less likely to show evidence of such modifications than bulk tissue. In this sense, theory would suggest that phloem contents provide a better estimate of Δ of raw photosynthate than does bulk leaf tissue.

Another set of post-photosynthetic modifications have been attributed to transport into and out of the phloem during downward vertical transport. If these modifications reflected additions of photosynthate from shaded branches, they might improve our estimates of whole-canopy photosynthesis. However, if they were due to leakage and refilling with an isotopic fractionation, then they would degrade our estimates (Gessler et al., 2009). In a detailed analysis of vertical changes in phloem composition in Scots pine at our site, we were unable to detect a vertical $\delta^{13}C$ gradient (data not shown). This argues that the isotope signal is preserved during transport.

Post-photosynthetic modifications may also result from chloroplast starch hydrolysis and phloem loading. Starch hydrolysis leads to diurnal changes in the isotopic composition of the sugars derived from it (Gessler et al., 2009). In one study, the sugars leaving the leaf in the phloem had nearly the same isotopic composition as the starch being hydrolyzed (Gessler et al., 2007). This result suggests that the photosynthates were not substantially altered upon phloem loading. On the other hand, some authors have found differences between $\delta^{13}C$ of leaf soluble organic matter and the sugars in the phloem (Brandes et al., 2006). This latter comparison assumes that the entire pool of leaf soluble organic matter is available for export and that insoluble compounds, like starch, are not used as substrate for export. If the assumption is true, it would suggest fractionation upon loading into the sieve tubes (Hobbie & Werner, 2004).

Isotopic changes in phloem contents could also arise from compound-specific isotopic signatures in the phloem. Such differences among compounds have been observed in phloem contents (Smith, Wild, Richter, Simonin, & Merchant, 2016) and they were especially noteworthy in the polyols in Douglas-fir xylem sap (Bögelein, Lehmann, & Thomas, 2019), which represented 37% of the phloem solutes and were approximately 2‰ more depleted than sucrose. It is not clear where the heavy carbon would go at polyol synthesis, but one might expect that it is retained in the substrates. Similarly, phloem sap contains N-compounds (e.g., amino acids and polyamines) as well. The $\delta^{13}C$ analysis of phloem contents allowed us to determine a C:N ratio, which was 119 ± 32 (SD) and 42 ± 20 in the R plot and the F plot, respectively. On both plots, the values were high enough to consider that non sugar compounds would have a small effect on the global isotopic signature. We acknowledge that a more detailed analysis would improve our predictions. In the meantime, we have assumed that the bulk fractionation is negligible.

Phloem contents must be used carefully before photosynthesis begins in spring. During this period before photosynthesis has begun, the phloem must contain, mobilized C reserves (Dubbert, Rascher, & Werner, 2012; Gessler et al., 2004). This would obviously not yield estimates of current WUE_i (Michelot, Eglin, Dufrêne, Lelarge-Trouverie, & Damesin, 2011). As soon as the environmental conditions improve in spring, stomatal conductance increases, the phloem fills with new photosynthates, and $\delta^{13}C_p$ begins to fall. This process may explain why $\delta^{13}C_p$ was highest outside the thermal growing season and decreased when photosynthetic activity recovered. Without correcting the WUE_i, the annual $GPP_{iso/SF}$ became too high for spring in a boreal forest (Saurer et al., 2014; Tang et al., 2014). The influence of these high values was reduced by the $\widehat{A}$ correction, which accounts for the reduction in photosynthetic rates at low temperatures.

4.2.3 | Sap flux estimate

Sap flux is a key variable in the $GPP_{iso/SF}$ approach in order to obtain transpiration. Although the technique describes temporal variation well, its use for quantitative estimates requires accounting for

several known sources of variation (Oren, Phillips, Katul, Ewers, & Pataki, 1998). Examples include sap flux trends radially in the stem (Cohen, Cohen, Cantuarias Aviles, & Schiller 2008; Ford, McGuire, Mitchell, & Teskey, 2004; Phillips, Oren, & Zimmermann, 1996; Renninger & Schäfer, 2012), azimuthally around the stem (Cohen et al., 2008; Oren, Phillips, Ewers, Pataki, & Megonigal, 1999), with tree size (Schäfer, Oren, & Tenhunen, 2000), and with local competition (Xiong et al., 2015). In addition, corrections are required when probe length exceeds the sapwood depth (Clearwater, Meinzer, Andrade, Goldstein, & Holbrook, 1999). Finally, the probes often require specific calibration (Steppe, De Pauw, Doody, & Teskey, 2010; Sun, Aubrey, & Teskey, 2012). Some corrections have been proposed to reduce uncertainties from random variation (Peters et al., 2018; Steppe et al., 2010; Sun et al., 2012), yet some tree-to-tree variation remains (Oren et al., 1998). The model we used to estimate transpiration was carefully built to account for these errors. It resulted from a careful measurement design at stand scale.

Tor-Ngern et al. (2017) began with high quality data based on careful accounting for radial and azimuthal variations and baseline corrections. They recognised that the sensors were not specifically calibrated for *P. sylvestris*, but the values agreed well with previously reported results and were robust to the errors induced by the probes (Lundblad, Lagergren, & Lindroth, 2001; Poyatos et al., 2007). Likewise the data were carefully scaled up to the stand using detailed descriptions of the allometric parameters and tree sizes (Ford et al., 2004; Oren et al., 1998). Because the sap flux/isotopic method is so dependent on quantitative sap flux data, other users must also ensure that their sap flux data remove any bias and are accurate as well as precise.

4.2.4 | High variability of VPD impacts on $g_{C\hat{A}}$

There was considerable variation in our estimate of $g_{C\hat{A}}$. Because $g_{C\hat{A}}$ was calculated as the ratio between transpiration and VPD, low VPD caused high variability and improbable $g_{C\hat{A}}$ results (Eqn. 6, Ewers, Oren, Johnsen, & Landsberg, 2001; Ewers & Oren, 2000). This was especially true in the early and late growing season. The same phenomenon occurred sporadically during the thermal growing season. It forced us to apply a filter and to replace the inconsistent data inside the thermal growing season by predictions from a simple regression between g_C and $\hat{A}$. This filtering and replacement is a common procedure, especially at high latitudes where VPD is low (Emberson et al., 2000; Tarvainen et al., 2015). Although we are satisfied with this solution for the moment, a better means of dealing with low VPD should be sought. One promising possibility is to use $\delta^{18}O$ to infer stomatal conductance under these conditions (Barbour, 2007); however, this requires that several ancillary measurements be made (Roden & Siegwolf, 2012).

4.3 | Mesophyll conductance influenced $GPP_{iso/SF}$ estimates

The calculation of WUE_i would not have been valid if g_m had been considered infinite (Seibt et al., 2008; Wingate et al., 2007). Yet g_m is still frequently ignored by some global photosynthesis models and ecophysiologists (Hu et al., 2010; Rogers et al., 2017; Zhao et al., 2005), or is embedded within a constant empirical adjustment (Cernusak et al., 2013) most likely due to the challenges in its measurements (Flexas et al., 2008; Pons et al., 2009). Likewise, the global modelling community has been reluctant to account for it because of the lack of consensus about how to measure or model it (Rogers, Medlyn, & Dukes 2014).

We compared three different ways of accounting for g_m. Simplest would be to assume a constant mean value (Keenan, Sabate, & Gracia, 2010). For example, we estimated GPP with a constant g_m = 0.31 mol CO_2 m^{-2} s^{-1} measured at the site (Stangl et al., 2019). The $GPP_{iso/SF}$ from the assumptions of g_m = 0.31 mol CO_2 m^{-2} s^{-1} was not different from the $GPP_{iso/SF}$ from the $g_{m\infty}$ assumption. Perhaps this is because the constant g_m value was estimated during sunny days in the summertime and therefore represents the maximal g_m, under optimal conditions.

We therefore based our comparison with PRELES on a constant ratio: $g_m/g_{C\hat{A}}$ = 2.67. The ratio has the advantage of allowing g_m to vary seasonally. Variation responds to environmental factors (Bickford, Hanson, & McDowell, 2010; Cano, López, & Warren, 2014; Han et al., 2016; Xiong, Douthe, & Flexas,

2018); both diurnal (Bickford, Hanson, & McDowell, 2010; Peguero-Pina et al., 2017; Stangl et al., 2019) and seasonal (Montpied, Granier, & Dreyer, 2009) variations have been reported. The use of a constant $g_m/g_{C\hat{A}}$ ratio was certainly artificial (Xiong, Douthe, & Flexas, 2018), but it is a relatively common assumption (Klein et al., 2016; Maseyk, Hemming, Anger, Leavitt, & Yakir, 2011). We suspect that the higher discrepancies between the $GPP_{iso/SF}$ and GPP_{PRELES} in the fall and to a lesser extent in the spring occurred because the constant ratio did not adequately account for seasonal dynamics in g_m. The need to refine our description of g_m is confirmed by the uncertainty analysis (Table S1 and Figure S3) The Sobol indices, which describe sources of uncertainty, showed that almost 75% of the $GPP_{iso/SF}$ uncertainty came from the $g_m/g_{C\hat{A}}$ estimate.

4.4 | Difference between fertilisation treatments

We found a slightly higher GPP in the fertilised plot than in the reference plots with the sap flux/isotopic method. Indeed, WUE_i in the F plot was higher than in the R plot, although $g_{C\hat{A}}$ was not different. This means that photosynthetic rates were higher on the F plot, as demonstrated in previous studies in coniferous boreal forest: photosynthetic activity, which is the product of g_S for CO_2 and the $[CO_2]$ gradient between the atmosphere and the sub stomatal chamber (C_a-C_i) increases only if the CO_2 gradient increases for a given g_S value (Duursma & Marshall, 2006; Marshall & Linder, 2013).

The difference between the F and the R plots was only significant at the daily time scale, perhaps because of the large number of repeated measurements (Table 2, Figure S5). However, this sap flux/isotopic result, corrected for autocorrelation, was validated with the daily PRELES estimates (Table 2, Figure S5). However, it should be recognized that these daily estimates are not independent and may exaggerate our ability to detect a difference. In contrast, the annual sums did not detect a difference (Figure 5), perhaps because we were able to compare only two years, limiting the power of ANOVA. Thus, our annual sums did not find a significantly higher GPP in the F plot compared to the R plot, agreeing with previous studies focused on photosynthetic activity at shoot (Tarvainen et al., 2016) and stand scale (Lim et al., 2015). The daily estimates did not agree. Based on these mixed results, we suggest that GPP under the F treatment might be slightly higher, but that a replicated study would be necessary to settle this question.

However, the magnitude of the GPP increase differed between PRELES and sap flux/isotopic methods. The 8% increase in $GPP_{iso/SF}$ due to fertilisation was nearest to Lim et al (2015), who inferred a 3% difference in GPP between the same F plot and the R plot based on biometric measurements. In contrast, the GPP_{PRELES} value in the F plot was 16% higher than in the R plot, almost twice the increase estimated from $GPP_{iso/SF}$ and five times higher than in Lim et al. (2015).

4.5 | Role of understorey species

A key difference between the GPP methods is that $GPP_{iso/SF}$ quantified GPP of the trees only whereas GPP_{PRELES} quantified GPP of the whole ecosystem, which included understorey GPP. Understorey GPP was 41 g C m^{-2} in a 120-year-old Scots pine boreal forest (Kulmala et al., 2011) and 5% of the ecosystem GPP in mixed spruce-pine forest (Palmroth et al., 2019). PRELES estimated understorey GPP at our site to be 7 and 9% of the ecosystem GPP on the reference and the fertilised plots, respectively (Tian et al., under review.). In other words, this preliminary estimate of fertilisation treatment would induce 2% increase of understorey GPP. A direct comparison of tree GPP between the sap flux/isotopic and PRELES (GPP_{PRELES}-7% and 9%) method would lead to 1369 vs 1194 g C m^{-2} y^{-1} in the R plot and 1483 vs 1248 g C m^{-2} y^{-1} in the F plot. However, this estimate needs more replicates to confirm the understorey contribution to global GPP. As these methods continue to improve, it may become possible to solve for understorey GPP by difference. Note that if a next study shows that the fertilisation significantly increased understorey GPP, then $GPP_{iso/SF}$ would not detect it, but GPP_{PRELES} would. Future work should explore this possibility.

5 | Conclusions

The $GPP_{iso/SF}$ method provides an alternative empirical method to estimate forest stand GPP that is independent of eddy covariance (EC). We compared $GPP_{iso/SF}$ estimates from PRELES, a semi-empirical model parameterised with EC data. When annual means were compared across two years, the GPP

estimates from the two methods were not significantly different. Moreover, the annual means showed no effect of the fertiliser treatment. However, when compared using daily estimates, the fertilized plot was 8% higher than the reference plot. The annual comparison agrees with previous estimates on this site, the daily comparison does not. Future work will continue to explore this question (e.g., Tian et al., in review). Adjusting $GPP_{iso/SF}$ for g_m was necessary; we explored three alternatives for doing so. The inclusion of mesophyll conductance provides an empirical/mechanistic means of connecting isotopic measurements to gas-exchange measurements and $GPP_{iso/SF}$ provides a means of scaling from individual trees to tree stands and canopies. Finally, a critical advantage of the sap flux/isotope based method for estimating GPP is that its requirements for the terrain and atmospheric conditions are less restrictive than for EC measurements. It can be applied in complex terrain, complex canopy structure, and non-turbulent atmospheres.

ACKNOWLEDGMENTS

This work was supported by the Knut and Alice Wallenberg Foundation (#2015.0047). Antoine Vernay was funded by the Kempe foundation (SMK-1743). The authors thank the ecophysiological team of Forest Ecology and Management department (SLU) and researchers working on "Carbon and Water Branchpoints in Boreal Forests" project for their helpful comments. We thank the SLU stable isotope laboratory (SSIL) staff for isotopic analysis and SITES staff for their financial support and their help in the field and for providing data. Finally, we thank Dr Thomas Perot for his help with the statistical analyses. Financial support for Ram Oren was provided by the Erkko Visiting Professor Programme of the Jane and Aatos Erkko 375th Anniversary Fund through the University of Helsinki.

AUTHOR CONTRIBUTIONS

The experiment was designed by JDM and SL; JDM and AV conceived the ideas and designed the methodology for the model comparison; PT, MP, and ZRS collected the data; JC and MP analysed meteorological and EC data, RO and PT designed the transpiration model, JDM and AV proposed the sap flux/isotope method and made the cross analyses of the different models, AM and XT provided PRELES estimates and ZRS provided g_m data. AV and JDM wrote the manuscript. All the authors contributed critically to the drafts and gave final approval for publication.

CONFLICT OF INTEREST

The authors have no conflicts of interest.

REFERENCES

Alekseychik, P. K., Mammarella, I., Launiainen, S., Rannik, Ü., & Vesala, T. (2013). Evolution of the nocturnal decoupled layer in a pine forest canopy. *Agricultural and Forest Meteorology*, *174–175*, 15–27. https://doi.org/10.1016/j.agrformet.2013.01.011

Aubinet, M., Chermanne, B., Vandenhaute, M., Longdoz, B., Yernaux, M., & Laitat, E. (2001). Long term carbon dioxide exchange above a mixed forest in the Belgian Ardennes. *Agricultural and Forest Meteorology*, *108*(4), 293–315. https://doi.org/10.1016/S0168-1923(01)00244-1

Baldocchi, D. D. (2003). Assessing the eddy covariance technique for evaluating carbon dioxide exchange rates of ecosystems: Past, present and future. *Global Change Biology*, *9*(4), 479–492. https://doi.org/10.1046/j.1365-2486.2003.00629.x

Barbour, M. M. (2007). Stable oxygen isotope composition of plant tissue: A review. *Functional Plant Biology*, *34*(2), 83–94. https://doi.org/10.1071/FP06228

Barbour, M. M., Ryazanova, S., & Tcherkez, G. (2017). Respiratory effects on the carbon isotope discrimination near the compensation point. In G. Tcherkez & J. Ghashghaie (Eds.), *Plant Respiration: Metabolic Fluxes and Carbon Balance* (Vol. 43, pp. 143–160). Springer International Publishing. https://doi.org/10.1007/978-3-319-68703-2_7

Beer, C., Reichstein, M., Tomelleri, E., Ciais, P., Jung, M., Carvalhais, N., Rödenbeck, C., Arain, M. A., Baldocchi, D., Bonan, G. B., Bondeau, A., Cescatti, A., Lasslop, G., Lindroth, A., Lomas, M., Luyssaert, S., Margolis, H., Oleson, K. W., Roupsard, O., … Papale, D. (2010). Terrestrial

gross carbon dioxide uptake: Global distribution and covariation with climate. *Science*, *329*(5993), 834–838. https://doi.org/10.1126/science.1184984

Bickford, C. P., Hanson, D. T., & McDowell, N. G. (2010). Influence of diurnal variation in mesophyll conductance on modelled 13C discrimination: Results from a field study. *Journal of Experimental Botany*, *61*(12), 3223–3233. https://doi.org/10.1093/jxb/erq137

Bögelein, R., Lehmann, M. M., & Thomas, F. M. (2019). Differences in carbon isotope leaf-to-phloem fractionation and mixing patterns along a vertical gradient in mature European beech and Douglas fir. *New Phytologist*, *222*(4), 1803–1815. https://doi.org/10.1111/nph.15735

Bowling, D. R., Pataki, D. E., & Randerson, J. T. (2008). Carbon isotopes in terrestrial ecosystem pools and CO2 fluxes. *New Phytologist*, *178*(1), 24–40. https://doi.org/10.1111/j.1469-8137.2007.02342.x

Brandes, E., Kodama, N., Whittaker, K., Weston, C., Rennenberg, H., Keitel, C., Adams, M. A., & Gessler, A. (2006). Short-term variation in the isotopic composition of organic matter allocated from the leaves to the stem of Pinus sylvestris: Effects of photosynthetic and postphotosynthetic carbon isotope fractionation. *Global Change Biology*, *12*(10), 1922–1939. https://doi.org/10.1111/j.1365-2486.2006.01205.x

Busch, F. A., Holloway-Phillips, M., Stuart-Williams, H., & Farquhar, G. D. (2020). Revisiting carbon isotope discrimination in C 3 plants shows respiration rules when photosynthesis is low. *Nature Plants*, *6*(3), 245–258. https://doi.org/10.1038/s41477-020-0606-6

Campbell, J. E., Berry, J. A., Seibt, U., Smith, S. J., Montzka, S. A., Launois, T., Belviso, S., Bopp, L., & Laine, M. (2017). Large historical growth in global terrestrial gross primary production. *Nature*, *544*(7648), 84–87. https://doi.org/10.1038/nature22030

Cano, F. J., López, R., & Warren, C. R. (2014). Implications of the mesophyll conductance to CO2 for photosynthesis and water-use efficiency during long-term water stress and recovery in two contrasting Eucalyptus species. *Plant, Cell & Environment*, *37*(11), 2470–2490. https://doi.org/10.1111/pce.12325

Cernusak, L. A., Ubierna, N., Winter, K., Holtum, J. A. M., Marshall, J. D., & Farquhar, G. D. (2013). Environmental and physiological determinants of carbon isotope discrimination in terrestrial plants. *New Phytologist*, *200*(4), 950–965. https://doi.org/10.1111/nph.12423

Cernusak, Lucas A., Tcherkez, G., Keitel, C., Cornwell, W. K., Santiago, L. S., Knohl, A., Barbour, M. M., Williams, D. G., Reich, P. B., Ellsworth, D. S., Dawson, T. E., Griffiths, H. G., Farquhar, G. D., & Wright, I. J. (2009). Why are non-photosynthetic tissues generally 13C enriched compared with leaves in C3 plants? Review and synthesis of current hypotheses. *Functional Plant Biology*, *36*(3), 199–213. https://doi.org/10.1071/FP08216

Clearwater, M. J., Meinzer, F. C., Andrade, J. L., Goldstein, G., & Holbrook, N. M. (1999). Potential errors in measurement of nonuniform sap flow using heat dissipation probes. *Tree Physiology*, *19*(10), 681–687. https://doi.org/10.1093/treephys/19.10.681

Cleveland, W., Grosse, E., & Shyu, W. (1992). Local regression models. Chapter 8 in Statistical models in S (JM Chambers and TJ Hastie eds.), 608 p. *Wadsworth & Brooks/Cole, Pacific Grove, CA*.

Cohen, Y., Cohen, S., Cantuarias-Aviles, T., & Schiller, G. (2008). Variations in the radial gradient of sap velocity in trunks of forest and fruit trees. *Plant and Soil*, *305*(1), 49–59. https://doi.org/10.1007/s11104-007-9351-0

Curtis, P. S., Hanson, P. J., Bolstad, P., Barford, C., Randolph, J. C., Schmid, H. P., & Wilson, K. B. (2002). Biometric and eddy-covariance based estimates of annual carbon storage in five eastern North American deciduous forests. *Agricultural and Forest Meteorology*, *113*(1), 3–19. https://doi.org/10.1016/S0168-1923(02)00099-0

Du, E., Terrer, C., Pellegrini, A. F. A., Ahlström, A., Lissa, C. J. van, Zhao, X., Xia, N., Wu, X., & Jackson, R. B. (2020). Global patterns of terrestrial nitrogen and phosphorus limitation. *Nature Geoscience*, 1–6. https://doi.org/10.1038/s41561-019-0530-4

Dubbert, M., Rascher, K. G., & Werner, C. (2012). Species-specific differences in temporal and spatial variation in δ13C of plant carbon pools and dark-respired CO2 under changing environmental conditions. *Photosynthesis Research*, *113*(1), 297–309. https://doi.org/10.1007/s11120-012-9748-3

Duursma, R. A., Kolari, P., Perämäki, M., Pulkkinen, M., Mäkelä, A., Nikinmaa, E., Hari, P., Aurela, M., Berbigier, P., Bernhofer, C., Grünwald, T., Loustau, D., Mölder, M., Verbeeck, H., & Vesala, T. (2009). Contributions of climate, leaf area index and leaf physiology to variation in gross primary production of six coniferous forests across Europe: A model-based analysis. *Tree Physiology*, *29*(5), 621–639. https://doi.org/10.1093/treephys/tpp010

Duursma, R. A., & Marshall, J. D. (2006). Vertical canopy gradients in δ13C correspond with leaf nitrogen content in a mixed-species conifer forest. *Trees*, *20*(4), 496–506. https://doi.org/10.1007/s00468-006-0065-3

Ehleringer, J., Hall, A., & Farquhar, G. (1993). Introduction: Water use in relation to productivity. *Stable Isotopes and Plant Carbon-Water Relations. Academic Press, New York*, 3–8.

Ehman, J. L., Schmid, H. P., Grimmond, C. S. B., Randolph, J. C., Hanson, P. J., Wayson, C. A., & Cropley, F. D. (2002). An initial intercomparison of micrometeorological and ecological inventory estimates of carbon exchange in a mid-latitude deciduous forest. *Global Change Biology*, *8*(6), 575–589. https://doi.org/10.1046/j.1365-2486.2002.00492.x

Emberson, L. D., Wieser, G., & Ashmore, M. R. (2000). Modelling of stomatal conductance and ozone flux of Norway spruce: Comparison with field data. *Environmental Pollution*, *109*(3), 393–402. https://doi.org/10.1016/S0269-7491(00)00042-7

Evans, J. R., & Caemmerer, S. V. (2013). Temperature response of carbon isotope discrimination and mesophyll conductance in tobacco. *Plant, Cell & Environment*, *36*(4), 745–756. https://doi.org/10.1111/j.1365-3040.2012.02591.x

Ewers, B E, Oren, R., Johnsen, K. H., & Landsberg, J. J. (2001). Estimating maximum mean canopy stomatal conductance for use in models. *Canadian Journal of Forest Research*, *31*(2), 198–207. https://doi.org/10.1139/x00-159

Ewers, Brent E., & Oren, R. (2000). Analyses of assumptions and errors in the calculation of stomatal conductance from sap flux measurements. *Tree Physiology*, *20*(9), 579–589. https://doi.org/10.1093/treephys/20.9.579

Farquhar, G. D., & Wong, S. C. (1984). An empirical model of stomatal conductance. *Functional Plant Biology*, *11*(3), 191–210. https://doi.org/10.1071/pp9840191

Farquhar, G., O'Leary, M., & Berry, J. (1982). On the relationship between carbon isotope discrimination and the intercellular carbon dioxide concentration in leaves. *Functional Plant Biology*, *9*(2), 121. https://doi.org/10.1071/PP9820121

Flexas, J., Díaz-Espejo, A., Conesa, M. A., Coopman, R. E., Douthe, C., Gago, J., Gallé, A., Galmés, J., Medrano, H., Ribas-Carbo, M., Tomàs, M., & Niinemets, Ü. (2016). Mesophyll conductance to CO2 and Rubisco as targets for improving intrinsic water use efficiency in C3 plants. *Plant, Cell & Environment*, *39*(5), 965–982. https://doi.org/10.1111/pce.12622

Flexas, J., Ribas-Carbó, M., Diaz-Espejo, A., Galmés, J., & Medrano, H. (2008). Mesophyll conductance to CO2: Current knowledge and future prospects. *Plant, Cell & Environment*, *31*(5), 602–621. https://doi.org/10.1111/j.1365-3040.2007.01757.x

Ford, C. R., McGuire, M. A., Mitchell, R. J., & Teskey, R. O. (2004). Assessing variation in the radial profile of sap flux density in Pinus species and its effect on daily water use. *Tree Physiology*, *24*(3), 241–249. https://doi.org/10.1093/treephys/24.3.241

Gessler, A., Rennenberg, H., & Keitel, C. (2004). Stable isotope composition of organic compounds transported in the phloem of european beech—Evaluation of different methods of phloem sap collection and assessment of gradients in carbon isotope composition during leaf-to-stem transport. *Plant Biology*, *6*(6), 721–729. https://doi.org/10.1055/s-2004-830350

Gessler A., Keitel C., Kodama N., Weston C., Winters A.J., Keith H., … Farquhar G.D. (2007) $\delta^{13}C$ of organic matter transported from the leaves to the roots in *Eucalyptus delegatensis*: short-term variations and relation to respired CO_2. *Functional Plant Biology 34(8)*, 692–706

Gessler, A, Tcherkez, G., Peuke, A. D., Ghashghaie, J., & Farquhar, G. D. (2008). Experimental evidence for diel variations of the carbon isotope composition in leaf, stem and phloem sap organic matter in Ricinus communis. *Plant, Cell & Environment*, *31*(7), 941–953. https://doi.org/10.1111/j.1365-3040.2008.01806.x

Gessler A., Brandes E., Buchmann N., Helle G., Rennenberg H. & Barnard R.L. (2009) Tracing carbon and oxygen isotope signals from newly assimilated sugars in the leaves to the tree-ring archive. *Plant, Cell & Environment 32(7)*, 780–795. 10.1111/j.1365-3040.2009.01957.x

Granier, A. (1985). Une nouvelle méthode pour la mesure du flux de sève brute dans le tronc des arbres. *Annales Des Sciences Forestieres*, *42*(2), 193–200.
Granier, A. (1987). Evaluation of transpiration in a Douglas-fir stand by means of sap flow measurements. *Tree Physiology*, *3*(4), 309–320. https://doi.org/10.1093/treephys/3.4.309
Granier, A., Loustau, D., & Bréda, N. (2000). A generic model of forest canopy conductance dependent on climate, soil water availability and leaf area index. *Annals of Forest Science*, *57*(8), 755–765. https://doi.org/10.1051/forest:2000158
Han, J.-M., Meng, H.-F., Wang, S.-Y., Jiang, C.-D., Liu, F., Zhang, W.-F., & Zhang, Y.-L. (2016). Variability of mesophyll conductance and its relationship with water use efficiency in cotton leaves under drought pretreatment. *Journal of Plant Physiology*, *194*, 61–71. https://doi.org/10.1016/j.jplph.2016.03.014
Hänninen, H. (2016). Climatic adaptation of boreal and temperate tree species. In H. Hänninen (Ed.), *Boreal and temperate trees in a changing climate: Modelling the ecophysiology of seasonality* (AV.tp-00604; pp. 1–13). Springer Netherlands. https://doi.org/10.1007/978-94-017-7549-6_1
Hasselquist, N. J., Metcalfe, D. B., Marshall, J. D., Lucas, R. W., & Högberg, P. (2016). Seasonality and nitrogen supply modify carbon partitioning in understory vegetation of a boreal coniferous forest. *Ecology*, *97*(3), 671–683. https://doi.org/10.1890/15-0831
Hasselquist, Niles J., Metcalfe, D. B., & Högberg, P. (2012). Contrasting effects of low and high nitrogen additions on soil CO2 flux components and ectomycorrhizal fungal sporocarp production in a boreal forest. *Global Change Biology*, *18*(12), 3596–3605. https://doi.org/10.1111/gcb.12001
Hobbie, E. A., & Werner, R. A. (2004). Intramolecular, compound-specific, and bulk carbon isotope patterns in C3 and C4 plants: A review and synthesis. *New Phytologist*, *161*(2), 371–385. https://doi.org/10.1111/j.1469-8137.2004.00970.x
Högberg, P. (2007). Environmental science: Nitrogen impacts on forest carbon. *Nature*, *447*(7146), 781–782. https://doi.org/10.1038/447781a
Hu, J., Moore, D. J. P., Riveros-Iregui, D. A., Burns, S. P., & Monson, R. K. (2010). Modeling whole-tree carbon assimilation rate using observed transpiration rates and needle sugar carbon isotope ratios. *New Phytologist*, *185*(4), 1000–1015. https://doi.org/10.1111/j.1469-8137.2009.03154.x
Hultine, K. R., Bush, S. E., West, A. G., Burtch, K. G., Pataki, D. E., & Ehleringer, J. R. (2008). Gender-specific patterns of aboveground allocation, canopy conductance and water use in a dominant riparian tree species: Acer negundo. *Tree Physiology*, *28*(9), 1383–1394. https://doi.org/10.1093/treephys/28.9.1383
Jocher, G., Marshall, J., Nilsson, M. B., Linder, S., Simon, G. D., Hörnlund, T., Lundmark, T., Näsholm, T., Ottosson Löfvenius, M., Tarvainen, L., Wallin, G., & Peichl, M. (2018). Impact of canopy decoupling and subcanopy advection on the annual carbon balance of a boreal Scots pine forest as derived from eddy covariance. *Journal of Geophysical Research: Biogeosciences*, *123*(2), 303–325. https://doi.org/10.1002/2017JG003988
Jocher, G., Ottosson Löfvenius, M., De Simon, G., Hörnlund, T., Linder, S., Lundmark, T., Marshall, J., Nilsson, M. B., Näsholm, T., Tarvainen, L., Öquist, M., & Peichl, M. (2017). Apparent winter CO2 uptake by a boreal forest due to decoupling. *Agricultural and Forest Meteorology*, *232*, 23–34. https://doi.org/10.1016/j.agrformet.2016.08.002
Kätterer, T., Andrén, O., & Jansson, P.-E. (2006). Pedotransfer functions for estimating plant available water and bulk density in Swedish agricultural soils. *Acta Agriculturae Scandinavica, Section B — Soil & Plant Science*, *56*(4), 263–276. https://doi.org/10.1080/09064710500310170
Keenan, T. F., Migliavacca, M., Papale, D., Baldocchi, D., Reichstein, M., Torn, M., & Wutzler, T. (2019). Widespread inhibition of daytime ecosystem respiration. *Nature Ecology & Evolution*, *3*(3), 407–415. https://doi.org/10.1038/s41559-019-0809-2
Keenan, T., Sabate, S., & Gracia, C. (2010). Soil water stress and coupled photosynthesis–conductance models: Bridging the gap between conflicting reports on the relative roles of stomatal, mesophyll conductance and biochemical limitations to photosynthesis. *Agricultural and Forest Meteorology*, *150*(3), 443–453. https://doi.org/10.1016/j.agrformet.2010.01.008

Kim, H.-S., Oren, R., & Hinckley, T. M. (2008). Actual and potential transpiration and carbon assimilation in an irrigated poplar plantation. *Tree Physiology*, *28*(4), 559–577. https://doi.org/10.1093/treephys/28.4.559

Klein, T., Rotenberg, E., Tatarinov, F., & Yakir, D. (2016). Association between sap flow-derived and eddy covariance-derived measurements of forest canopy CO2 uptake. *New Phytologist*, *209*(1), 436–446. https://doi.org/10.1111/nph.13597

Kolari, P., Pumpanen, J., Rannik, Ü., Ilvesniemi, H., Hari, P., & Berninger, F. (2004). Carbon balance of different aged Scots pine forests in Southern Finland. *Global Change Biology*, *10*(7), 1106–1119. https://doi.org/10.1111/j.1529-8817.2003.00797.x

Kulmala, L., Pumpanen, J., Kolari, P., Muukkonen, P., Hari, P., & Vesala, T. (2011). Photosynthetic production of ground vegetation in different-aged Scots pine (Pinus sylvestris) forests. *Canadian Journal of Forest Research*, *41*(10), 2020–2030. https://doi.org/10.1139/x11-121

Lagergren, F., Lindroth, A., Dellwik, E., Ibrom, A., Lankreijer, H., Launiainen, S., Mölder, M., Kolari, P., Pilegaard, K., & Vesala, T. (2008). Biophysical controls on CO2 fluxes of three Northern forests based on long-term eddy covariance data. *Tellus B: Chemical and Physical Meteorology*, *60*(2), 143–152. https://doi.org/10.1111/j.1600-0889.2007.00324.x

Laudon, H., Taberman, I., Ågren, A., Futter, M., Ottosson-Löfvenius, M., & Bishop, K. (2013). The Krycklan catchment study—A flagship infrastructure for hydrology, biogeochemistry, and climate research in the boreal landscape. *Water Resources Research*, *49*(10), 7154–7158. https://doi.org/10.1002/wrcr.20520

Lim, H., Oren, R., Palmroth, S., Tor-ngern, P., Mörling, T., Näsholm, T., Lundmark, T., Helmisaari, H.-S., Leppälammi-Kujansuu, J., & Linder, S. (2015). Inter-annual variability of precipitation constrains the production response of boreal Pinus sylvestris to nitrogen fertilization. *Forest Ecology and Management*, *348*, 31–45. https://doi.org/10.1016/j.foreco.2015.03.029

Linderholm, H. W. (2006). Growing season changes in the last century. *Agricultural and Forest Meteorology*, *137*(1), 1–14. https://doi.org/10.1016/j.agrformet.2006.03.006

Lundblad, M., Lagergren, F., & Lindroth, A. (2001). Evaluation of heat balance and heat dissipation methods for sapflow measurements in pine and spruce. *Annals of Forest Science*, *58*(6), 625–638. https://doi.org/10.1051/forest:2001150

Magnani, F., Mencuccini, M., Borghetti, M., Berbigier, P., Berninger, F., Delzon, S., Grelle, A., Hari, P., Jarvis, P. G., Kolari, P., Kowalski, A. S., Lankreijer, H., Law, B. E., Lindroth, A., Loustau, D., Manca, G., Moncrieff, J. B., Rayment, M., Tedeschi, V., … Grace, J. (2007). The human footprint in the carbon cycle of temperate and boreal forests. *Nature*, *447*(7146), 849–851. https://doi.org/10.1038/nature05847

Mäkelä, A., Hari, P., Berninger, F., Hänninen, H., & Nikinmaa, E. (2004). Acclimation of photosynthetic capacity in Scots pine to the annual cycle of temperature. *Tree Physiology*, *24*(4), 369–376. https://doi.org/10.1093/treephys/24.4.369

Mäkelä, A., Kolari, P., Karimäki, J., Nikinmaa, E., Perämäki, M., & Hari, P. (2006). Modelling five years of weather-driven variation of GPP in a boreal forest. *Agricultural and Forest Meteorology*, *139*(3), 382–398. https://doi.org/10.1016/j.agrformet.2006.08.017

Mäkelä, A., Pulkkinen, M., Kolari, P., Lagergren, F., Berbigier, P., Lindroth, A., Loustau, D., Nikinmaa, E., Vesala, T., & Hari, P. (2008). Developing an empirical model of stand GPP with the LUE approach: Analysis of eddy covariance data at five contrasting conifer sites in Europe. *Global Change Biology*, *14*(1), 92–108. https://doi.org/10.1111/j.1365-2486.2007.01463.x

Marshall, J. D., & Linder, S. (2013). Mineral nutrition and elevated CO2 interact to modify delta C-13, an index of gas exchange, in Norway spruce. *Tree Physiology*, *33*(11), 1132–1144. https://doi.org/10.1093/treephys/tpt004

Marshall, J. D., & Waring, R. H. (1984). Conifers and broadleaf species: Stomatal sensitivity differs in western Oregon. *Canadian Journal of Forest Research*, *14*(6), 905–908. https://doi.org/10.1139/x84-161

Maseyk, K., Hemming, D., Angert, A., Leavitt, S. W., & Yakir, D. (2011). Increase in water-use efficiency and underlying processes in pine forests across a precipitation gradient in the dry Mediterranean region over the past 30 years. *Oecologia*, *167*(2), 573–585. https://doi.org/10.1007/s00442-011-2010-4

Medlyn, B. E., Dreyer, E., Ellsworth, D., Forstreuter, M., Harley, P. C., Kirschbaum, M. U. F., Roux, X. L., Montpied, P., Strassemeyer, J., Walcroft, A., Wang, K., & Loustau, D. (2002). Temperature response of parameters of a biochemically based model of photosynthesis. II. A review of experimental data. *Plant, Cell & Environment*, *25*(9), 1167–1179. https://doi.org/10.1046/j.1365-3040.2002.00891.x

Medlyn, Belinda E., Duursma, R. A., Eamus, D., Ellsworth, D. S., Prentice, I. C., Barton, C. V. M., Crous, K. Y., Angelis, P. D., Freeman, M., & Wingate, L. (2011). Reconciling the optimal and empirical approaches to modelling stomatal conductance. *Global Change Biology*, *17*(6), 2134–2144. https://doi.org/10.1111/j.1365-2486.2010.02375.x

Merchant, A., Buckley, T. N., Pfautsch, S., Turnbull, T. L., Samsa, G. A., & Adams, M. A. (2012). Site-specific responses to short-term environmental variation are reflected in leaf and phloem-sap carbon isotopic abundance of field grown Eucalyptus globulus. *Physiologia Plantarum*, *146*(4), 448–459. https://doi.org/10.1111/j.1399-3054.2012.01638.x

Michelot, A., Eglin, T., Dufrêne, E., Lelarge-Trouverie, C., & Damesin, C. (2011). Comparison of seasonal variations in water-use efficiency calculated from the carbon isotope composition of tree rings and flux data in a temperate forest. *Plant, Cell & Environment*, *34*(2), 230–244. https://doi.org/10.1111/j.1365-3040.2010.02238.x

Minunno, F., Peltoniemi, M., Launiainen, S., Aurela, M., Lindroth, A., Lohila, A., Mammarella, I., Minkkinen, K., & Mäkelä, A. (2016). Calibration and validation of a semi-empirical flux ecosystem model for coniferous forests in the Boreal region. *Ecological Modelling*, *341*, 37–52. https://doi.org/10.1016/j.ecolmodel.2016.09.020

Montpied, P., Granier, A., & Dreyer, E. (2009). Seasonal time-course of gradients of photosynthetic capacity and mesophyll conductance to CO2 across a beech (Fagus sylvatica L.) canopy. *Journal of Experimental Botany*, *60*(8), 2407–2418. https://doi.org/10.1093/jxb/erp093

Murray, F. (1967). On the computation of saturation vapor pressure. *Journal of Applied Meteorology*, *6*(1), 203–204.

Ngao, J., Adam, B., & Saudreau, M. (2017). Intra-crown spatial variability of leaf temperature and stomatal conductance enhanced by drought in apple tree as assessed by the RATP model. *Agricultural and Forest Meteorology*, *237–238*, 340–354. https://doi.org/10.1016/j.agrformet.2017.02.036

Offermann, C., Ferrio, J. P., Holst, J., Grote, R., Siegwolf, R., Kayler, Z., & Gessler, A. (2011). The long way down—Are carbon and oxygen isotope signals in the tree ring uncoupled from canopy physiological processes? *Tree Physiology*, *31*(10), 1088–1102. https://doi.org/10.1093/treephys/tpr093

Oren, R., Phillips, N., Ewers, B. E., Pataki, D. E., & Megonigal, J. P. (1999). Sap-flux-scaled transpiration responses to light, vapor pressure deficit, and leaf area reduction in a flooded Taxodium distichum forest. *Tree Physiology*, *19*(6), 337–347. https://doi.org/10.1093/treephys/19.6.337

Oren, Ram, Phillips, N., Katul, G., Ewers, B. E., & Pataki, D. E. (1998). Scaling xylem sap flux and soil water balance and calculating variance: A method for partitioning water flux in forests. *Annales Des Sciences Forestières*, *55*(1–2), 191–216. https://doi.org/10.1051/forest:19980112

Oren, Ram, Zimmermann, R., & Terbough, J. (1996). Transpiration in upper amazonia floodplain and upland forests in response to drought-breaking rains. *Ecology*, *77*(3), 968–973. https://doi.org/10.2307/2265517

Palmroth, S., Bach, L. H., Lindh, M., Kolari, P., Nordin, A., & Palmqvist, K. (2019). Nitrogen supply and other controls of carbon uptake of understory vegetation in a boreal Picea abies forest. *Agricultural and Forest Meteorology*, *276–277*, 107620. https://doi.org/10.1016/j.agrformet.2019.107620

Papale, D., Reichstein, M., Aubinet, M., Canfora, E., Bernhofer, C., Kutsch, W., Longdoz, B., Rambal, S., Valentini, R., Vesala, T., & Yakir, D. (2006). Towards a standardized processing of net ecosystem exchange measured with eddy covariance technique: Algorithms and uncertainty estimation. *Biogeosciences*, *3*(4), 571–583.

Peguero-Pina, J. J., Aranda, I., Cano, F. J., Galmés, J., Gil-Pelegrín, E., Niinemets, Ü., Sancho-Knapik, D., & Flexas, J. (2017). The role of mesophyll conductance in oak photosynthesis: Among- and within-species variability. In E. Gil-Pelegrín, J. J. Peguero-Pina, & D. Sancho-

Knapik (Eds.), *Oaks Physiological Ecology. Exploring the Functional Diversity of Genus Quercus L.* (pp. 303–325). Springer International Publishing. https://doi.org/10.1007/978-3-319-69099-5_9

Peichl, M., Brodeur, J. J., Khomik, M., & Arain, M. A. (2010). Biometric and eddy-covariance based estimates of carbon fluxes in an age-sequence of temperate pine forests. *Agricultural and Forest Meteorology*, *150*(7), 952–965. https://doi.org/10.1016/j.agrformet.2010.03.002

Peltoniemi, M., Pulkkinen, M., Aurela, M., Pumpanen, J., Kolari, P., & Mäkelä, A. (2015). A semi-empirical model of boreal-forest gross primary production, evapotranspiration, and soil water-calibration and sensitivity analysis. *Boreal Environment Research*, *20*, 151–171.

Peters, R. L., Fonti, P., Frank, D. C., Poyatos, R., Pappas, C., Kahmen, A., Carraro, V., Prendin, A. L., Schneider, L., Baltzer, J. L., Baron-Gafford, G. A., Dietrich, L., Heinrich, I., Minor, R. L., Sonnentag, O., Matheny, A. M., Wightman, M. G., & Steppe, K. (2018). Quantification of uncertainties in conifer sap flow measured with the thermal dissipation method. *New Phytologist*, *219*(4), 1283–1299. https://doi.org/10.1111/nph.15241

Phillips, N., Oren, R., & Zimmermann, R. (1996). Radial patterns of xylem sap flow in non-, diffuse- and ring-porous tree species. *Plant, Cell & Environment*, *19*(8), 983–990. https://doi.org/10.1111/j.1365-3040.1996.tb00463.x

Pinheiro, J., Bates, D., DebRoy, S., & Sarkar, D. (2016). R Core Team (2016) nlme: Linear and nonlinear mixed effects models. R Package Version 3.1-128. Available at ht tps. *Cran. r-Project. Org/Web/Packages/Nlme/Index. Html. Accessed July*, *7*.

Pons, T. L., Flexas, J., von Caemmerer, S., Evans, J. R., Genty, B., Ribas-Carbo, M., & Brugnoli, E. (2009). Estimating mesophyll conductance to CO2: Methodology, potential errors, and recommendations. *Journal of Experimental Botany*, *60*(8), 2217–2234. https://doi.org/10.1093/jxb/erp081

Poyatos, R., Martínez-Vilalta, J., Čermák, J., Ceulemans, R., Granier, A., Irvine, J., Köstner, B., Lagergren, F., Meiresonne, L., Nadezhdina, N., Zimmermann, R., Llorens, P., & Mencuccini, M. (2007). Plasticity in hydraulic architecture of Scots pine across Eurasia. *Oecologia*, *153*(2), 245–259. https://doi.org/10.1007/s00442-007-0740-0

R Core Team. (2016). *R: A Language and Environment for Statistical Computing*. R Foundation for Statistical Computing. https://www.R-project.org/

Rascher, K. G., Máguas, C., & Werner, C. (2010). On the use of phloem sap δ13C as an indicator of canopy carbon discrimination. *Tree Physiology*, *30*(12), 1499–1514. https://doi.org/10.1093/treephys/tpq092

Renninger, H. J., & Schäfer, K. V. R. (2012). Comparison of tissue heat balance- and thermal dissipation-derived sap flow measurements in ring-porous oaks and a pine. *Frontiers in Plant Science*, *3*, 103. https://doi.org/10.3389/fpls.2012.00103

Roden, J., & Siegwolf, R. (2012). Is the dual-isotope conceptual model fully operational? *Tree Physiology*, *32*(10), 1179–1182. https://doi.org/10.1093/treephys/tps099

Rogers, A., Medlyn, B. E., & Dukes, J. S. (2014). Improving representation of photosynthesis in Earth System Models. *New Phytologist*, *204*(1), 12–14. https://doi.org/10.1111/nph.12972

Rogers, A., Medlyn, B. E., Dukes, J. S., Bonan, G., Caemmerer, S. von, Dietze, M. C., Kattge, J., Leakey, A. D. B., Mercado, L. M., Niinemets, Ü., Prentice, I. C., Serbin, S. P., Sitch, S., Way, D. A., & Zaehle, S. (2017). A roadmap for improving the representation of photosynthesis in Earth system models. *New Phytologist*, *213*(1), 22–42. https://doi.org/10.1111/nph.14283

Saltelli, A., Ratto, M., Andres, T., Campolongo, F., Cariboni, J., Gatelli, D., Saisana, M., & Tarantola, S. (2008). *Global Sensitivity Analysis: The Primer*. John Wiley & Sons.

Saurer, M., Spahni, R., Frank, D. C., Joos, F., Leuenberger, M., Loader, N. J., McCarroll, D., Gagen, M., Poulter, B., Siegwolf, R. T. W., Andreu-Hayles, L., Boettger, T., Liñán, I. D., Fairchild, I. J., Friedrich, M., Gutierrez, E., Haupt, M., Hilasvuori, E., Heinrich, I., … Young, G. H. F. (2014). Spatial variability and temporal trends in water-use efficiency of European forests. *Global Change Biology*, *20*(12), 3700–3712. https://doi.org/10.1111/gcb.12717

Schäfer, K. V. R., Oren, R., Ellsworth, D. S., Lai, C.-T., Herrick, J. D., Finzi, A. C., Richter, D. D., & Katul, G. G. (2003). Exposure to an enriched CO2 atmosphere alters carbon assimilation and allocation in a pine forest ecosystem. *Global Change Biology*, *9*(10), 1378–1400. https://doi.org/10.1046/j.1365-2486.2003.00662.x

Schäfer, K. V. R., Oren, R., & Tenhunen, J. D. (2000). The effect of tree height on crown level stomatal conductance. *Plant, Cell & Environment*, *23*(4), 365–375. https://doi.org/10.1046/j.1365-3040.2000.00553.x

Schneider, S., GEßLER, A., Weber, P., Sengbusch, D. V., Hanemann, U., & Rennenberg, H. (1996). Soluble N compounds in trees exposed to high loads of N: A comparison of spruce (Picea abies) and beech (Fagus sylvatica) grown under field conditions. *New Phytologist*, *134*(1), 103–114. https://doi.org/10.1111/j.1469-8137.1996.tb01150.x

Seibt, U., Rajabi, A., Griffiths, H., & Berry, J. A. (2008). Carbon isotopes and water use efficiency: Sense and sensitivity. *Oecologia*, *155*(3), 441–454. https://doi.org/10.1007/s00442-007-0932-7

Smith, M., Wild, B., Richter, A., Simonin, K., & Merchant, A. (2016). Carbon isotope composition of carbohydrates and polyols in leaf and phloem sap of *Phaseolus vulgaris* L. influences predictions of plant water use efficiency. *Plant and Cell Physiology*, *57*(8), 1756–1766. https://doi.org/10.1093/pcp/pcw099

Stangl, Z. R., Tarvainen, L., Wallin, G., Ubierna, N., Räntfors, M., & Marshall, J. D. (2019). Diurnal variation in mesophyll conductance and its influence on modelled water-use efficiency in a mature boreal Pinus sylvestris stand. *Photosynthesis Research*, *141*(1), 53–63. https://doi.org/10.1007/s11120-019-00645-6

Steppe, K., De Pauw, D. J. W., Doody, T. M., & Teskey, R. O. (2010). A comparison of sap flux density using thermal dissipation, heat pulse velocity and heat field deformation methods. *Agricultural and Forest Meteorology*, *150*(7), 1046–1056. https://doi.org/10.1016/j.agrformet.2010.04.004

Sun, H., Aubrey, D. P., & Teskey, R. O. (2012). A simple calibration improved the accuracy of the thermal dissipation technique for sap flow measurements in juvenile trees of six species. *Trees*, *26*(2), 631–640. https://doi.org/10.1007/s00468-011-0631-1

Tang, X., Li, H., Desai, A. R., Nagy, Z., Luo, J., Kolb, T. E., Olioso, A., Xu, X., Yao, L., Kutsch, W., Pilegaard, K., Köstner, B., & Ammann, C. (2014). How is water-use efficiency of terrestrial ecosystems distributed and changing on Earth? *Scientific Reports*, *4*(1), 1–11. https://doi.org/10.1038/srep07483

Tarvainen, L., Lutz, M., Räntfors, M., Näsholm, T., & Wallin, G. (2016). Increased needle nitrogen contents did not improve shoot photosynthetic performance of mature nitrogen-poor Scots pine trees. *Frontiers in Plant Science*, *7*, 1051. https://doi.org/10.3389/fpls.2016.01051

Tarvainen, L., Räntfors, M., & Wallin, G. (2015). Seasonal and within-canopy variation in shoot-scale resource-use efficiency trade-offs in a Norway spruce stand. *Plant, Cell & Environment*, *38*(11), 2487–2496. https://doi.org/10.1111/pce.12565

Tcherkez, G., Gauthier, P., Buckley, T. N., Busch, F. A., Barbour, M. M., Bruhn, D., Heskel, M. A., Gong, X. Y., Crous, K. Y., Griffin, K., Way, D., Turnbull, M., Adams, M. A., Atkin, O. K., Farquhar, G. D., & Cornic, G. (2017). Leaf day respiration: Low CO2 flux but high significance for metabolism and carbon balance. *New Phytologist*, *216*(4), 986–1001. https://doi.org/10.1111/nph.14816

Thomas, C. K., Martin, J. G., Law, B. E., & Davis, K. (2013). Toward biologically meaningful net carbon exchange estimates for tall, dense canopies: Multi-level eddy covariance observations and canopy coupling regimes in a mature Douglas-fir forest in Oregon. *Agricultural and Forest Meteorology*, *173*, 14–27. https://doi.org/10.1016/j.agrformet.2013.01.001

Tian, X., Minunno, F., Cao, T., Peltoniemi, M., Kalliokoski, T., & Mäkelä, A. (2020). Extending the range of applicability of the semi-empirical ecosystem flux model PRELES for varying forest types and climate. *Global Change Biology*, *n/a*(n/a), 1–21. https://doi.org/10.1111/gcb.14992

Tor-Ngern, P., Oren, R., Oishi, A. C., Uebelherr, J. M., Palmroth, S., Tarvainen, L., Ottosson-Löfvenius, M., Linder, S., Domec, J.-C., & Näsholm, T. (2017). Ecophysiological variation of transpiration of pine forests: Synthesis of new and published results. *Ecological Applications*, *27*(1), 118–133. https://doi.org/10.1002/eap.1423

Tuzet, A., Perrier, A., & Leuning, R. (2003). A coupled model of stomatal conductance, photosynthesis and transpiration. *Plant, Cell & Environment*, *26*(7), 1097–1116. https://doi.org/10.1046/j.1365-3040.2003.01035.x

Ubierna, N., & Marshall, J. D. (2011). Estimation of canopy average mesophyll conductance using δ13C of phloem contents. *Plant, Cell & Environment*, *34*(9), 1521–1535. https://doi.org/10.1111/j.1365-3040.2011.02350.x

Warren, C. R. (2008). Stand aside stomata, another actor deserves centre stage: The forgotten role of the internal conductance to CO2 transfer. *Journal of Experimental Botany*, *59*(7), 1475–1487. https://doi.org/10.1093/jxb/erm245

Warren, C. R., & Adams, M. A. (2006). Internal conductance does not scale with photosynthetic capacity: Implications for carbon isotope discrimination and the economics of water and nitrogen use in photosynthesis. *Plant, Cell & Environment*, *29*(2), 192–201. https://doi.org/10.1111/j.1365-3040.2005.01412.x

Wehr, R., Munger, J. W., McManus, J. B., Nelson, D. D., Zahniser, M. S., Davidson, E. A., Wofsy, S. C., & Saleska, S. R. (2016). Seasonality of temperate forest photosynthesis and daytime respiration. *Nature*, *534*(7609), 680–683. https://doi.org/10.1038/nature17966

Werner, R. A., Buchmann, N., Siegwolf, R. T. W., Kornexl, B. E., & Gessler, A. (2011). Metabolic fluxes, carbon isotope fractionation and respiration – lessons to be learned from plant biochemistry. *New Phytologist*, *191*(1), 10–15. https://doi.org/10.1111/j.1469-8137.2011.03741.x

Werner, C., Schnyder, H., Cuntz, M., Keitel, C., Zeeman, M. J., Dawson, T. E., Badeck, F.-W., Brugnoli, E., Ghashghaie, J., Grams, T. E. E., Kayler, Z. E., Lakatos, M., Lee, X., Máguas, C., Ogée, J., Rascher, K. G., Siegwolf, R. T. W., Unger, S., Welker, J., … Gessler, A. (2012). Progress and challenges in using stable isotopes to trace plant carbon and water relations across scales. *Biogeosciences*, *9*(8), 3083. https://doi:10.5194/bgd-8-2659-2011

Wingate, L., Seibt, U., Moncrieff, J. B., Jarvis, P. G., & Lloyd, J. (2007). Variations in 13C discrimination during CO2 exchange by Picea sitchensis branches in the field. *Plant, Cell & Environment*, *30*(5), 600–616. https://doi.org/10.1111/j.1365-3040.2007.01647.x

Wohlfahrt, G., & Gu, L. (2015). The many meanings of gross photosynthesis and their implication for photosynthesis research from leaf to globe. *Plant, Cell & Environment*, *38*(12), 2500–2507. https://doi.org/10.1111/pce.12569

Xiong, D., Douthe, C., & Flexas, J. (2018). Differential coordination of stomatal conductance, mesophyll conductance, and leaf hydraulic conductance in response to changing light across species. *Plant, Cell & Environment*, *41*(2), 436–450. https://doi.org/10.1111/pce.13111

Xiong, W., Oren, R., Wang, Y., Yu, P., Liu, H., Cao, G., Xu, L., Wang, Y., & Zuo, H. (2015). Heterogeneity of competition at decameter scale: Patches of high canopy leaf area in a shade-intolerant larch stand transpire less yet are more sensitive to drought. *Tree Physiology*, *35*(5), 470–484. https://doi.org/10.1093/treephys/tpv022

Zha, T., Xing, Z., Wang, K.-Y., Kellomäki, S., & Barr, A. G. (2007). Total and component carbon fluxes of a Scots pine ecosystem from chamber measurements and eddy covariance. *Annals of Botany*, *99*(2), 345–353. https://doi.org/10.1093/aob/mcl266

Zhao, P., Lu, P., Ma, L., Sun, G., Rao, X., Cai, X., & Zeng, X. (2005). Combining sap flow measurement-based canopy stomatal conductance and 13C discrimination to estimate forest carbon assimilation. *Chinese Science Bulletin*, *50*(18), 2021–2027. https://doi.org/10.1007/BF03322795

Zweifel, R., Eugster, W., Etzold, S., Dobbertin, M., Buchmann, N., & Häsler, R. (2010). Link between continuous stem radius changes and net ecosystem productivity of a subalpine Norway spruce forest in the Swiss Alps. *New Phytologist*, *187*(3), 819–830. https://doi.org/10.1111/j.1469-8137.2010.03301.x

Table 1. Abbreviations, definitions and units of all variables used in the study

Abbreviations	Definitions	units	Constant values
A	Assimilation rate	g C m^{-2} d^{-1}	
a_a	Fractionation during diffusion through air	‰	4.4
a_i	Fractionation during diffusion through water	‰	1.8
b	Fractionation during carboxylation	‰	29
c_1	Coefficient of proportionality	m^3 mol^{-1} °C	0.0367
C_a	Ambient CO_2 concentration	ppm	
C_i	Internal CO_2 concentration	ppm	
E_{cd}	Transpiration rate at stand level	mm d^{-1}	
E_{cdmax}	Maximal transpiration rate at stand level	mm d^{-1}	
f	Fractionation during photorespiration	‰	16.2
g_m	Internal conductance	mol m^{-2} s^{-1}	
$g_{m\infty}$	Infinite value of g_i	mol m^{-2} s^{-1}	∞
g_C	Stomatal conductance at stand level	mol H_2O m^{-2} d^{-1}	
$g_{C\hat{A}}$	Stomatal conductance at stand level corrected by $\hat{\alpha}$	mol H_2O m^{-2} d^{-1}	
GPP	Gross primary production	g C m^{-2} d^{-1}	
GPP_{EC}	Gross primary production estimated by eddy-covariance	g C m^{-2} d^{-1}	
$GPP_{iso/SF}$	Gross primary production estimated by combined method with isotopic data and sapflow measurements	g C m^{-2} d^{-1}	
GPP_{PRELES}	Gross primary production estimated by PRELES model	g C m^{-2} d^{-1}	
LAI	Leaf Area Index	m^2 m^{-2}	
M_C	Molar mass of carbon	g mol^{-1}	12
M_{H2O}	Molar mass of water	g mol^{-1}	18
n_D	Number of day light hours	NA	
P_{145}	Atmospheric pressure at 145m a.s.l	kPa	99.6
PPFD	Photosynthetic photon flux density	mol m^{-2} d^{-1}	
R	Universal gas constant	J mol^{-1} K^{-1}	8.314
r	Ratio of diffusivities of CO_2 and water vapour in the air	NA	1.6
R_d	Daytime respiration	g C m^{-2} d^{-1}	
REW	Relative extractable water	NA	
RH	Relative humidity	%	
S(t)	State of photosynthetic acclimation (°C) at time t (day)	°C	
S_0	Threshold value of the photosynthetic state of acclimation	°C	-5.33
SWC_{FC}	Soil water content at field capacity	m^3 m^{-3}	
SWC_t	Soil water content at sampling time	m^3 m^{-3}	
SWC_{WP}	Soil water content at wilting point	m^3 m^{-3}	
T_a	Ambient temperature	°C	
T_K	Temperature	K	
VPD_D	Day light mean VPD	kPa	
VPD_Z	Normalised VPD	kPa	
WUE_i	Intrinsic water use efficiency	ppm	
$\hat{A}$	Photosynthetic capacity	°C	
$\hat{A}_{max}$	Maximal photosynthetic capacity	°C	
Δ	Observed carbon discrimination during gas-exchange	‰	
$\delta^{13}C_a$	Ratio of heavy to light ^{13}C isotope in the air	‰	
$\delta^{13}C_p$	Ratio of heavy to light ^{13}C isotope in phloem content	‰	
Γ^*	CO_2 compensation point	µmol mol^{-1}	
τ	Time constant	day	8.23

Table 2 Coefficients of the linear regression (corrected for autocorrelation) between daily GPP in the fertilised plot vs daily GPP in the reference plot across methods and years (slope (a) and intercept (b) ± SE).·,*, **, *** correspond to $p < 0.1$, 0.05, 0.01 and 0.001, respectively, after t-test when comparing the slope of the regressions with 1:1 regression.

		2012			2013		
Method	g_m assumptions	a	b	R^2	a	b	R^2
$GPP_{iso/SF}$	$g_m/g_{C\hat{A}} = 2.67$	1.06 (± 0.008)***	0.05 (± 0.04)	0.98	1.10 (± 0.01)***	0.04 (± 0.05)	0.98
	$g_m = 0.31$	1.07 (± 0.006)***	0.04 (± 0.04)	0.99	1.03 (± 0.008)***	0.08 (± 0.05)	0.98
	$g_{m\infty}$	1.06 (± 0.006)***	0.05 (± 0.04)	0.99	0.97 (± 0.01)***	0.27 (± 0.07)***	0.96
GPP_{PRELES}		1.15 (± 1^E-6)***	-3^E-6 (± 3^E-6)	0.99	1.16 (± 0.001)***	0.01 (± 0.006)	0.99

Figure captions

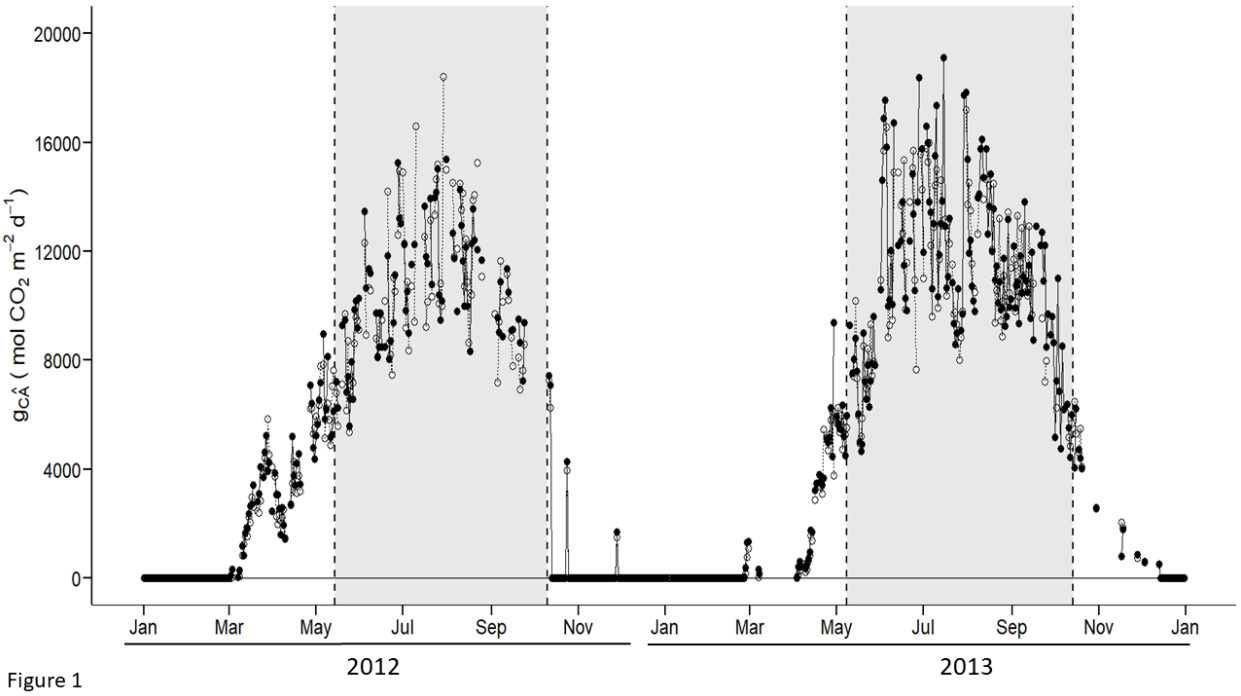

Figure 1

FIGURE 1: Canopy conductance corrected by $\widehat{A}$ for the fertilised (black circles and, solid lines) and the reference (white circles, dashed lines) plots in 2012 and 2013. Grey areas represent the thermal growing seasons

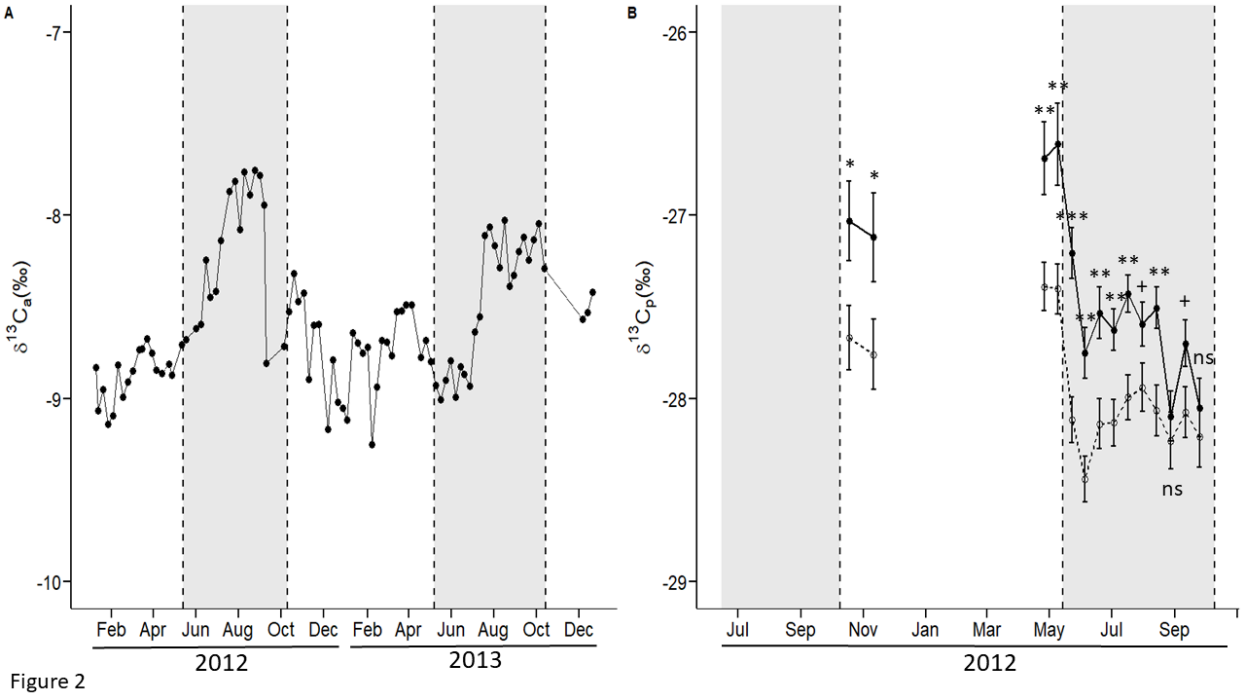

Figure 2

FIGURE 2: Atmospheric $\delta^{13}C_a$ signature in 2012 and 2013 (A) and phloem $\delta^{13}C_p$ signature in 2012 (B) ± SE (n = 15). ns, +, *, **, *** correspond to $p \geq 0.1$, $p < 0.1$, 0.05, 0.01 and 0.001, respectively, after pairwise comparison between the F plot and the R plot for each date. Grey areas represent the thermal growing seasons. The fertilised plot is represented in black circles and solid line and the reference plot in white circles and dotted line

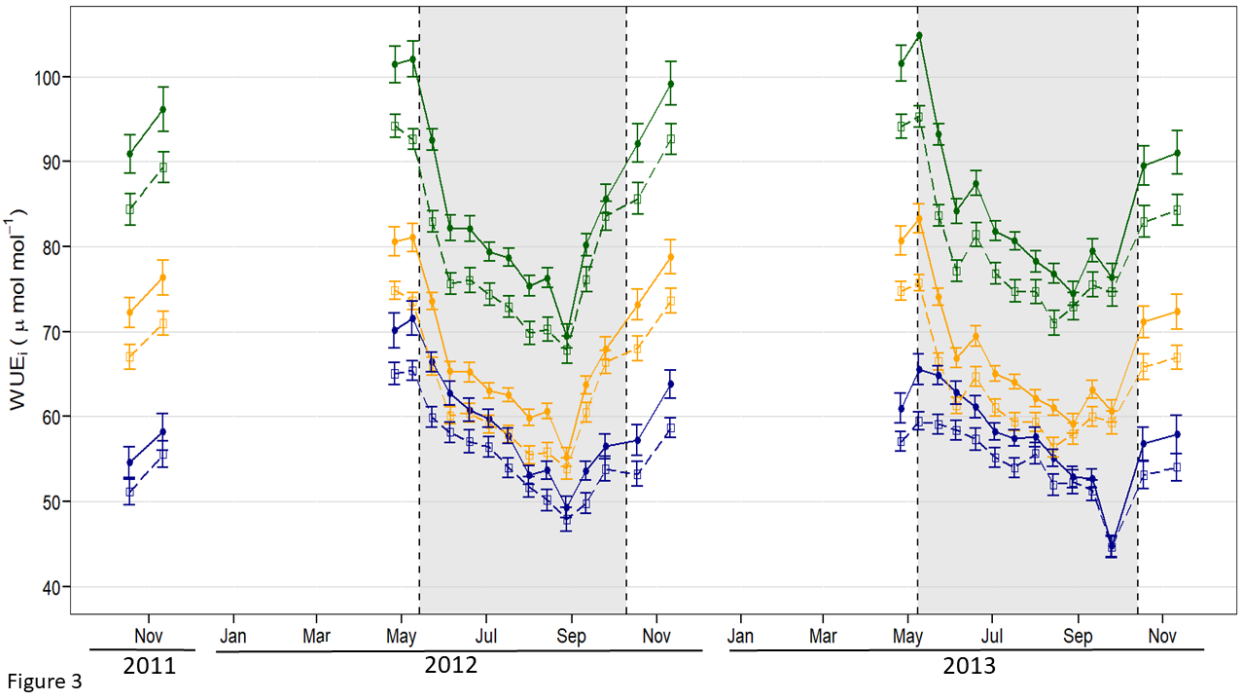

Figure 3

FIGURE 3: Intrinsic water use efficiency at stand level (WUE_i) for fertilised (filled circles and solid line) and reference plot (empty squares and dashed line) in 2012 and 2013, assuming a $g_{m\infty}$ assumption (green), a $g_m/g_{C\hat{A}} = 2.67$ assumption (yellow) or a $g_m = 0.31$ mol CO_2 m^{-2} s^{-1} assumption (blue). Grey areas represent the thermal growing season Statistical results comparing WUE_i between fertilised and reference plots: *** correspond to $p < 0.001$, respectively, after anova.

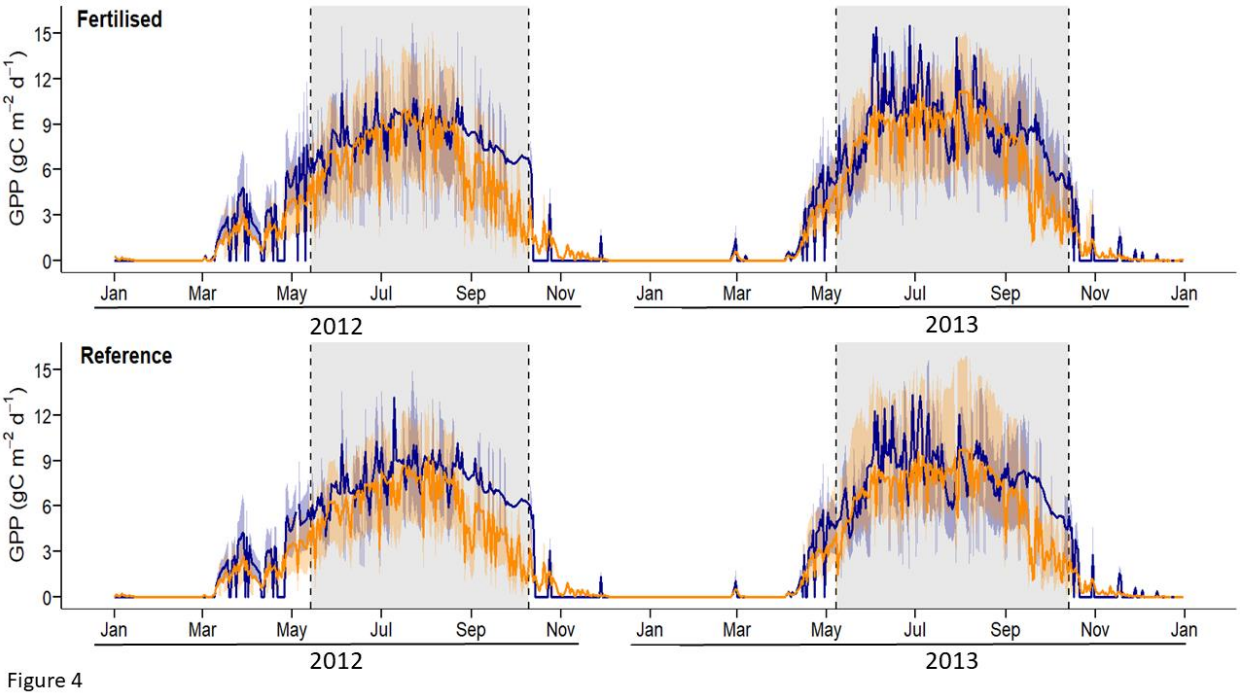

Figure 4

FIGURE 4: Daily GPP_{PRELES} (orange) and $GPP_{iso/SF}$ (blue) in the fertilised plot (upper row) and in the reference plot (lower row). Shaded areas around the curves represent the Monte Carlo uncertainties. The shaded boxes represent the thermal growing seasons.

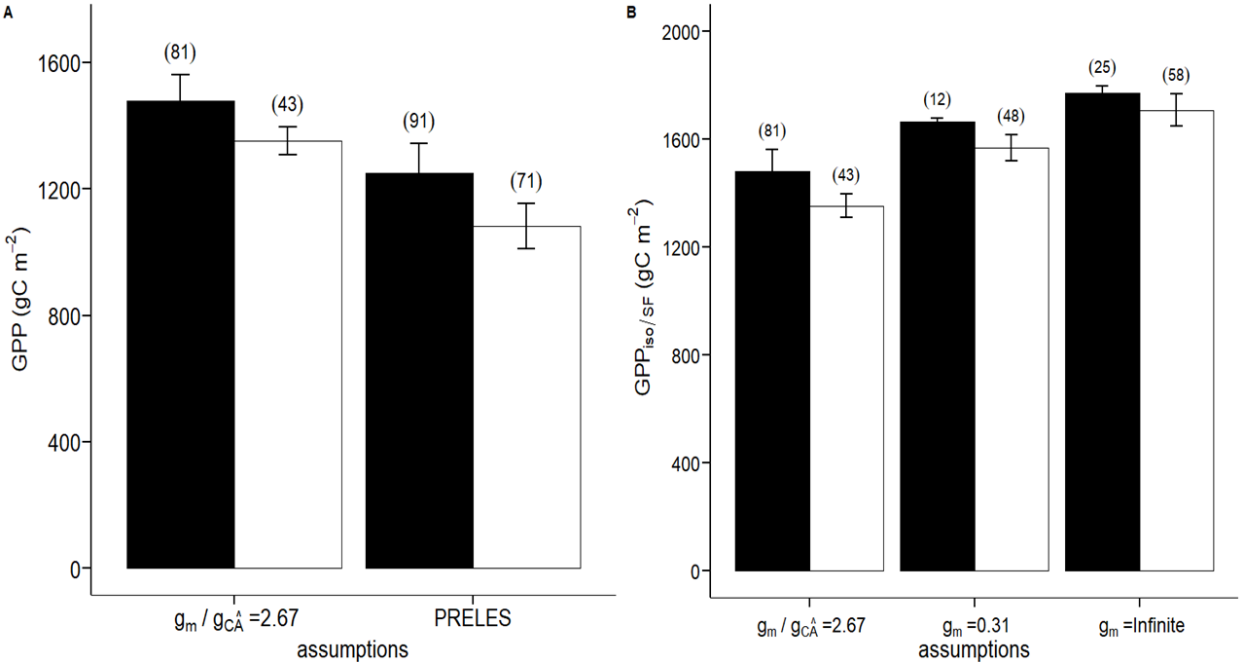

Figure 5

FIGURE 5: Annual sum of GPP for sap flux/isotopic (mean 2012 and 2013) method corrected by $\hat{\alpha}$ considering the g_m assumption, $g_m/g_{C\hat{A}}$ = 2.67 and PRELES (A) or considering the g_m assumption, g_m= 0.31 mol CO_2 m^{-2} s^{-1} and g_m infinite (B). Black bars correspond to the fertilized plot and the white bar to

the reference plot. Errors bars correspond to standard deviation and their values are in brackets. Letters shows the statistical differences ($\alpha = 0.05$) between the treatment combinations (modelling approach × fertilisation treatment.

Supporting Information

Article title: **Estimating canopy gross primary production by combining phloem stable isotopes with canopy and mesophyll conductances**

Authors: Antoine Vernay[1], Xianglin Tian[2], Jinshu Chi[1], Sune Linder[3], Annikki Mäkelä[2], Ram Oren[2,4], Matthias Peichl[1], Zsofia R Stangl[1], Pantana Tor-Ngern[5,6], John D Marshall[1*]

FIGURE S1: Environmental data in Rosinedal in 2012 and 2013. Sum of daily precipitation (A), daily mean photosynthetic photon flux density (B), daily mean temperature (C) and daily VPD during day light hours (D) in the fertilised (F, black circle) and in the reference (R, white circle) plots, respectively. Grey areas represent the thermal growing season.

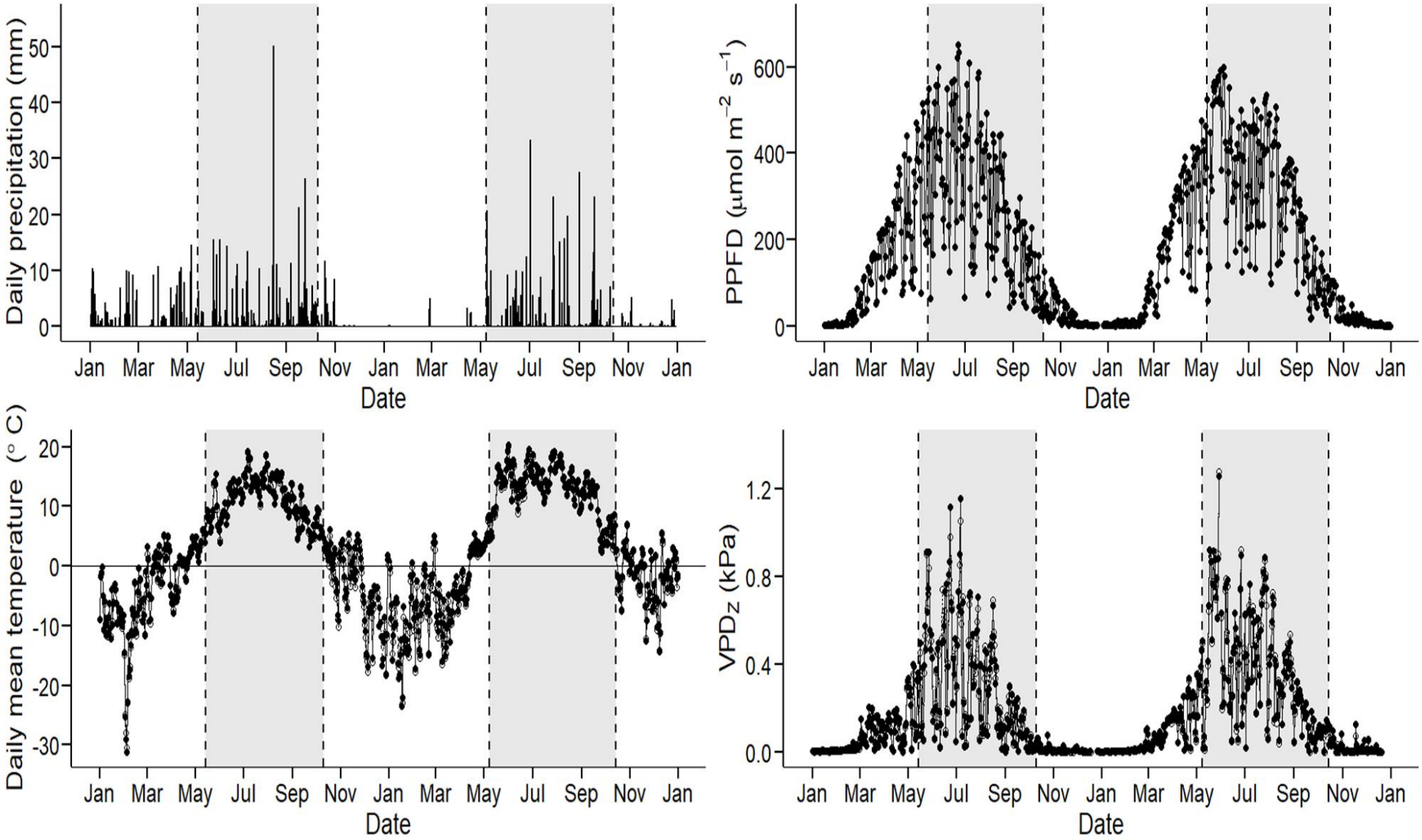

FIGURE S2: Variation of Δ values in 2012 and 2013. Black circle are the Δ calculated from $\delta^{13}C_p$ content. The solid line is the predicted values of Δ (grey area represents the 95% confidence interval)

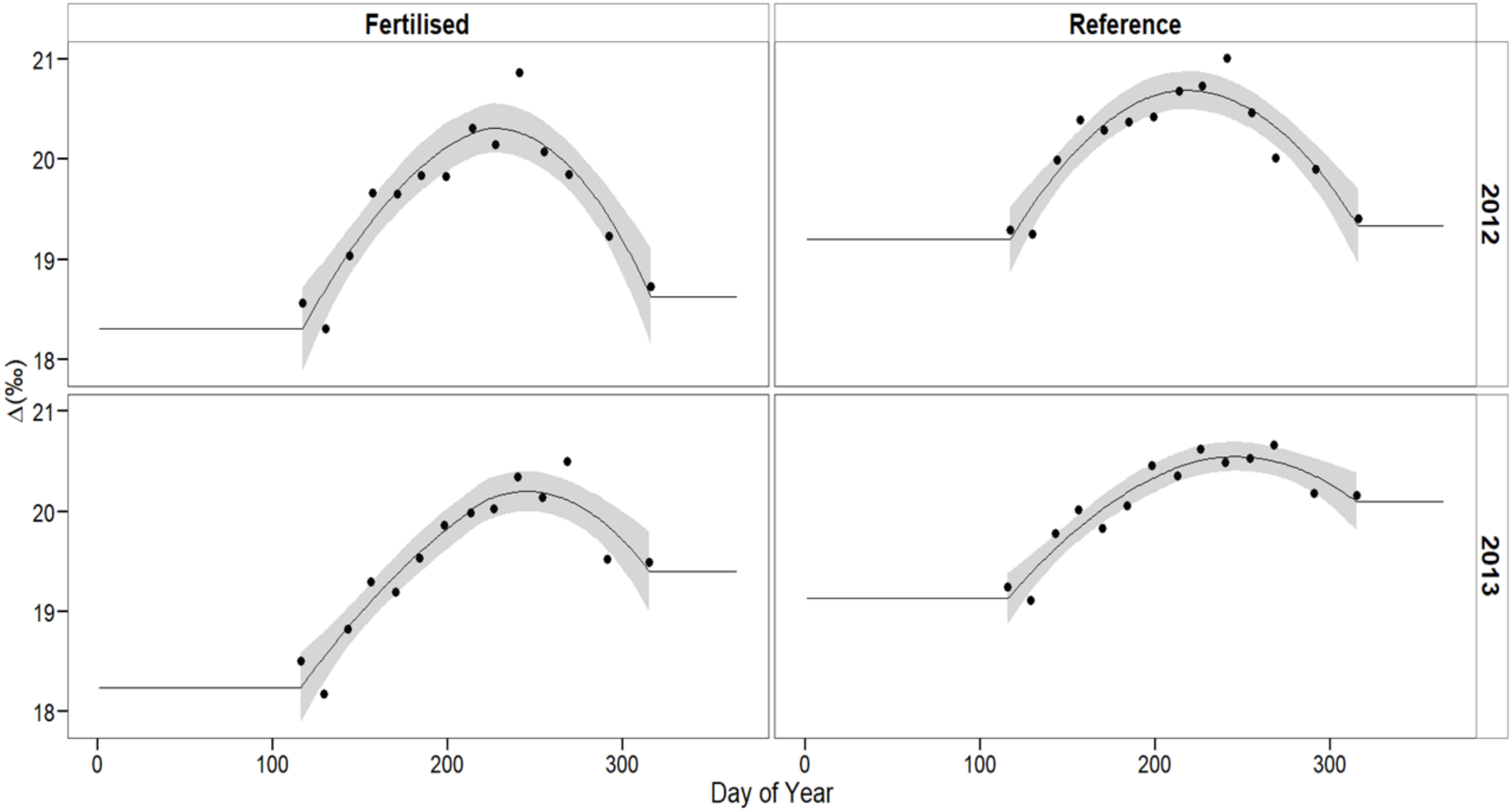

FIGURE S3: Uncertainty partitioning for sap flux/isotopic method between the potential error sources, Δ (grey), Γ* (red), E_{cd} (blue) and g_m/g_C (green)

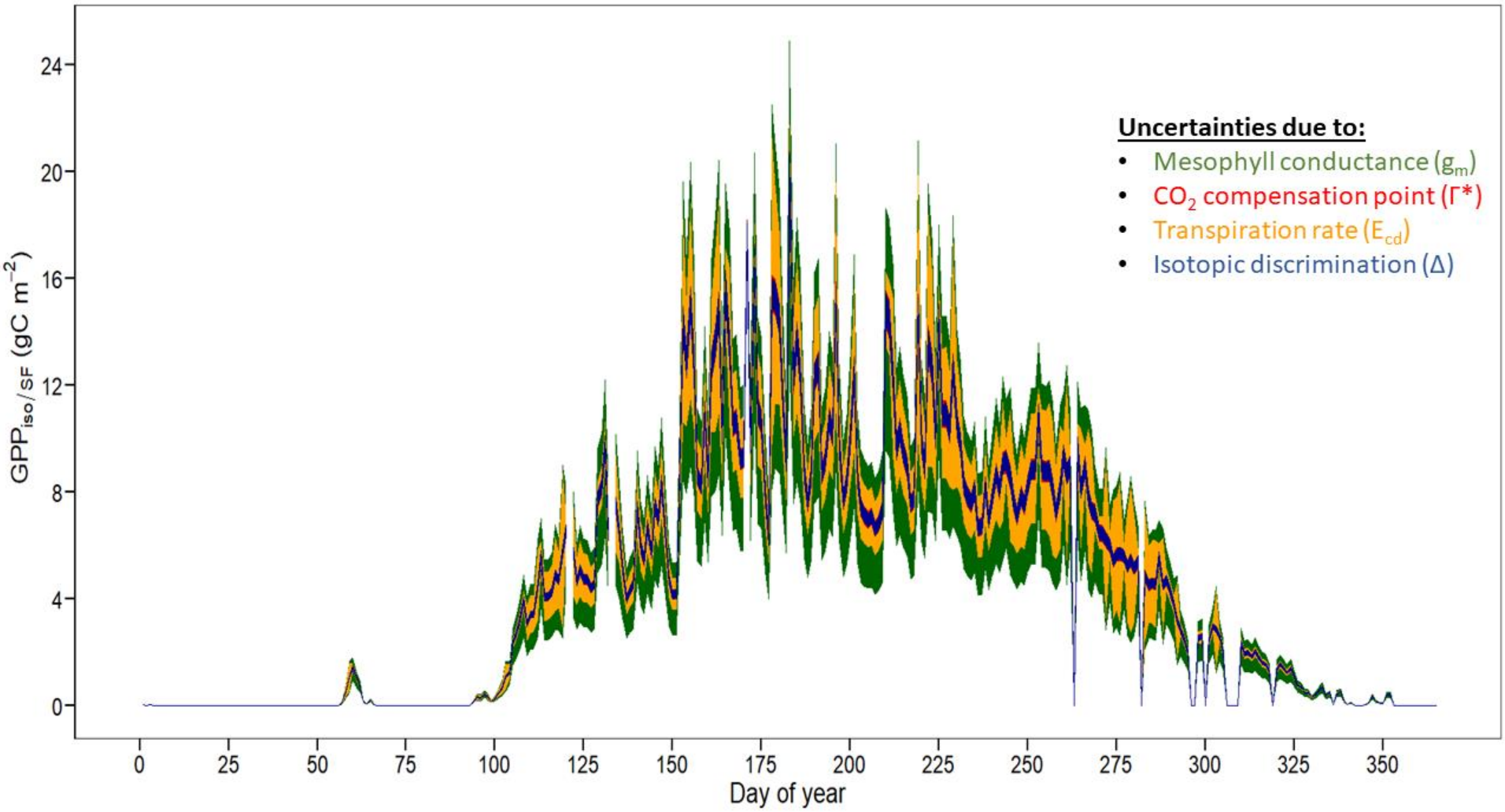

FIGURE S4: Daily $\hat{A}/\hat{A}_{max}$ in 2012 and 2013 in the fertilised (black circles and solid line) and the reference plots (white circle and dashed line). $\hat{A}_{max}$ was estimated as the mean $\hat{A}$ value measured in July 2012 and 2013, respectively.

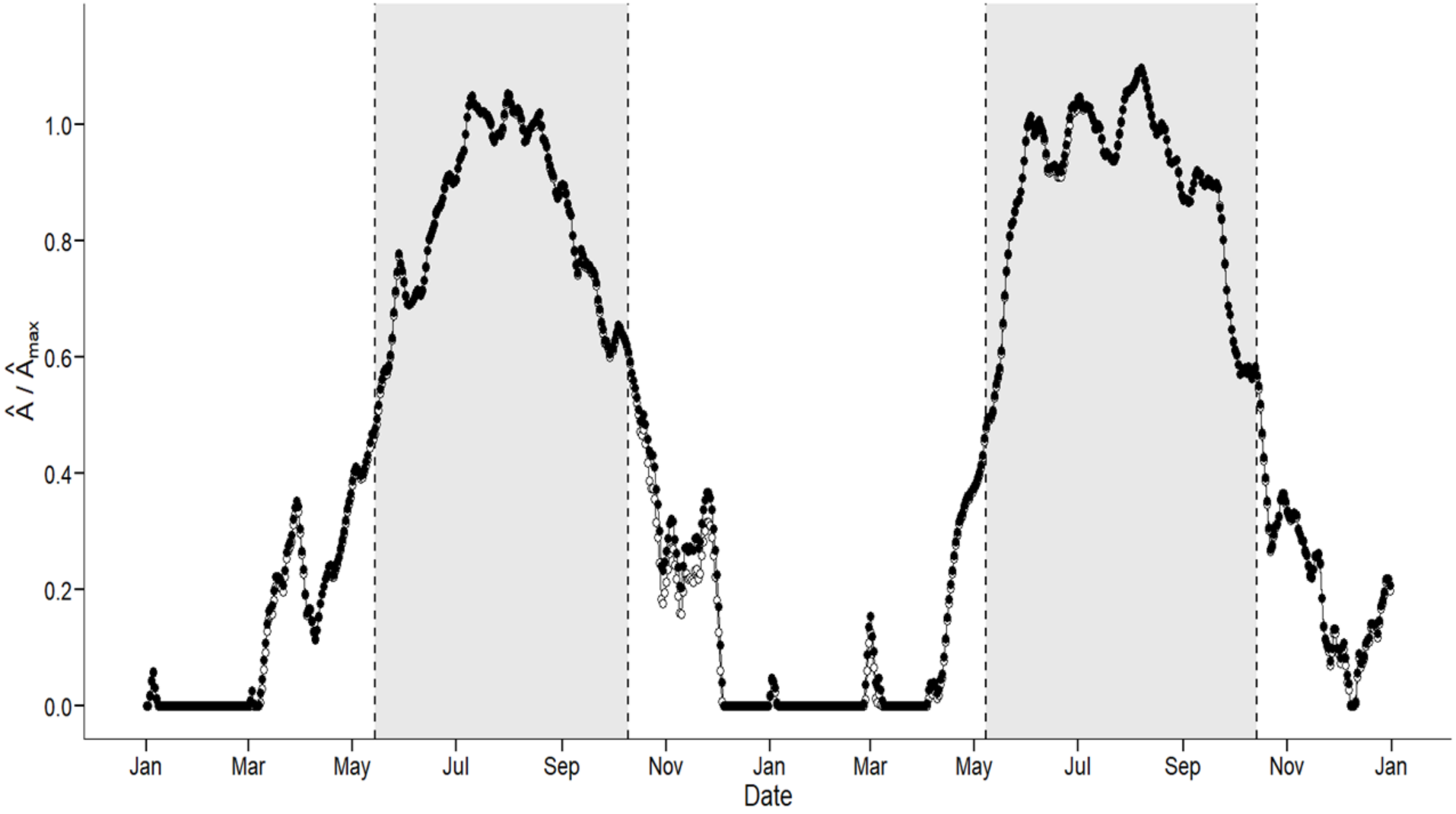

FIGURE S5 Spearman's correlation between the different methods estimating GPP. Values correspond to Spearman's coefficient. 2012 is represented on the left panel and 2013 on the right panel. $GPP_{iso/SF}$ values were calculated for $g_m/g_{C\hat{A}} = 2.67$ assumption.

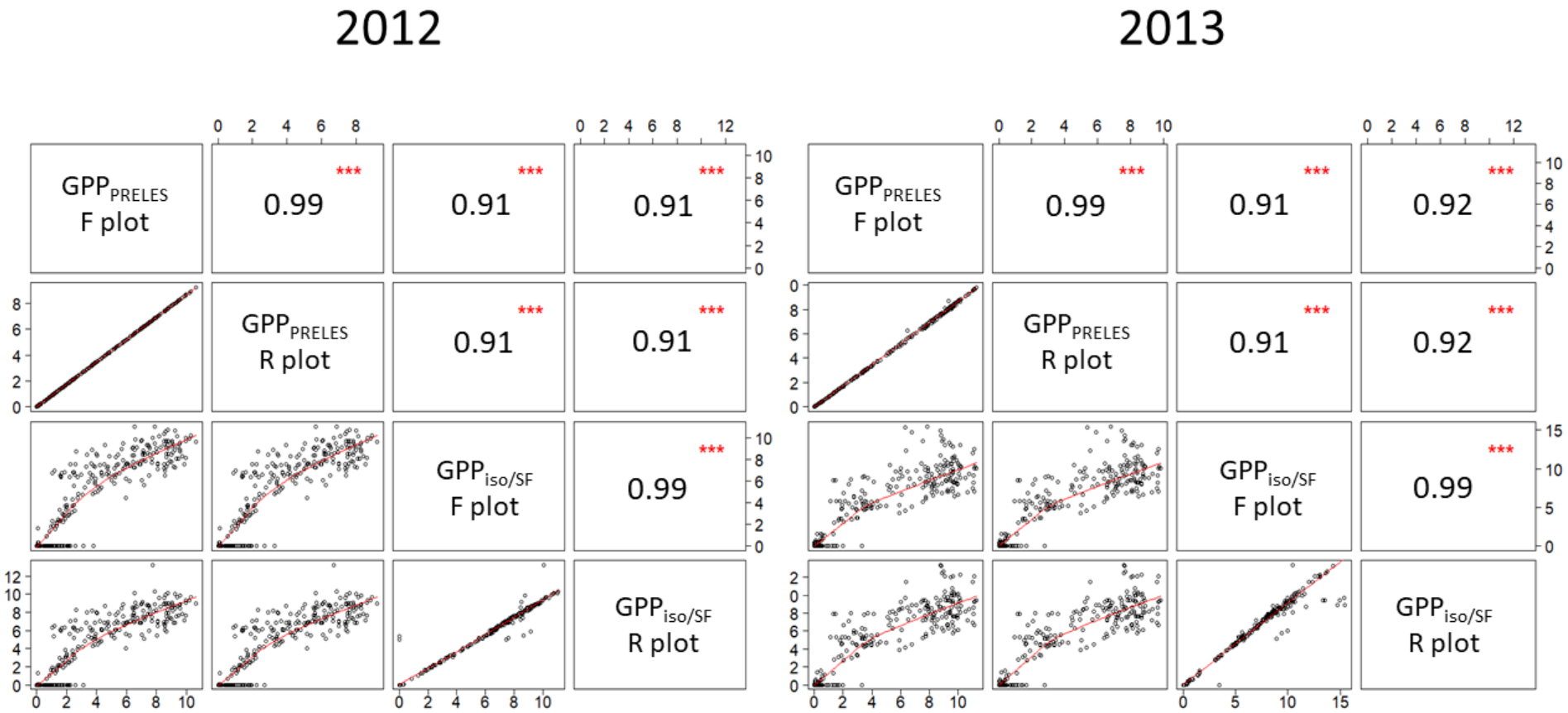

FIGURE S6: Comparison of GPP on the fertilised plot vs the reference plot in 2012 (green) and 2013 (grey) with $GPP_{iso/SF}$ for $g_m/g_{C\hat{A}}$ = 2.67 assumption (A), GPP_{PRELES} (B), $GPP_{iso/SF}$ for g_m = 0.31 mol CO_2 m^{-2} s^{-1} (C) and infinite g_m assumption (D). The black dashed line represents the 1:1 line.

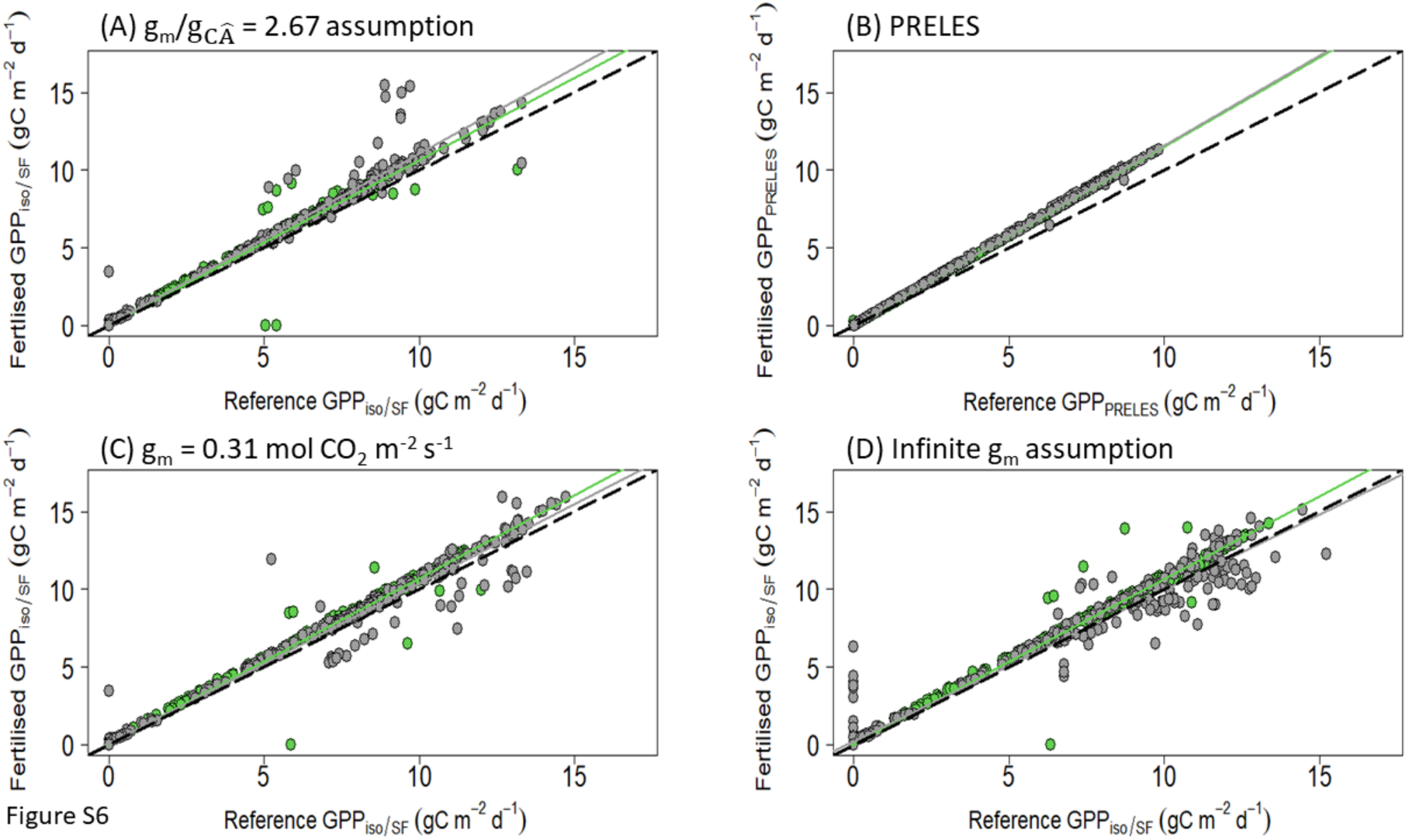

Figure S6

Table S1 Error distribution and associated Sobol indices

Sources of uncertainty	Error distribution	Reference	Sobol Indices
Δ	$\Delta \sim N(\mu = \Delta^{(M)}, \sigma = 0.1529)$	Field measurements and loess smoothing	0.9%
$\Gamma*$	$\Gamma * \sim N(\mu = \Gamma *^{(M)}, \sigma = 3.0)$	Bernacchi et al. (2001)	0.6%
Ecd	$Ecdmax \sim N\left(\mu = Ecdmax^{(M)}, \sigma = 0.10494\right), Ecdmax \in (0, +\infty)$ $Ecd \sim N(\mu = Ecd^{(M)}, \sigma = 0.04143), Ecd \in (0, +\infty)$	Tor-ngern et al. (2017)	24.6%
g_C/g_m	$\frac{g_c}{g_m} \sim N(\mu = \frac{1}{2.67}, \sigma = \frac{1}{2.7}), \frac{g_c}{g_m} \in (0,2]$	Stangl et al. (2019)	72.2%

Note: The superscript (M) means output from equations in the references. The sobol indices were the average being weighted by daily GPP values.